UNIVERSITÀ DEGLI STUDI DI PADOVA

DIPARTIMENTO DI INGEGNERIA INDUSTRIALE

CORSO DI LAUREA MAGISTRALE IN INGEGNERIA CHIMICA E DEI PROCESSI INDUSTRIALI

Tesi di Laurea Magistrale in
Ingegneria Chimica e dei Processi Industriali

Study of bi-solid mixture bed expansion and of elutriation from gas-solid dense fluidized bed

Relatore: *Prof. Paolo Canu*

Correlatore: *Prof. Renaud Ansart*

Laboratoire de Génie Chimique – Institut National Polytechnique de Toulouse

Laureanda: Silvia Palano

ANNO ACCADEMICO 2014-2015

Alla mia famiglia.

Acknowledgements

I would like to thank my French supervisor, Prof. Renaud Ansart, who welcomed me in the team, he helped me in carrying out my work, supported me and had patience in dealing with me. It was a pleasure to work together.

A special thanks goes to my Italian supervisors, Prof. Andrea Claudio Santomaso and Prof. Paolo Canu, who have followed my work from a distance and they have never been left me, especially this last who spurred me to realize this experience and never give up.

Last but not least thanks to Prof. Carmelo Sunseri who supported me in my choices and it is also thanks to him if I undertook this experience.

I also would like to thank all my friends and colleagues and all the people I met in this route.

Riassunto

Questa tesi è frutto di una collaborazione tra l'Università degli Studi di Padova e l'*Institut National Polytechnique de Toulouse*. Il lavoro è stato svolto presso i laboratori del *Laboratoire de Génie Chimique.*

Lo scopo di questo lavoro è lo studio del comportamento fluidodinamico all'interno di reattori gas-solido a letto fluidizzato contenenti particolato polidisperso. In particolar modo si è voluto approfondire il fenomeno dell'elutriazione, che si riscontra quando la velocità terminale dei solidi granulari trattati è inferiore alla velocità superficiale del gas. Quest'ultimo trascina le particelle più fini mentre quelle maggiori rimangono nel letto. L'elutriazione può avere dei connotati negativi, in quanto può determinare svantaggi per un processo sia a livello economico, sia per perdita di reagenti e/o prodotti. Per esempio nel caso di combustore o gassificatore si ha una diminuzione del diametro del *char*, e sotto una certa dimensione quest'ultimo viene perso nei fumi e quindi non convertito. Per contro l'elutriazione può essere sfruttata per separare specie diverse (esempio *ash* e *metal oxide*).

Dopo un'approfondita analisi dei dati di letteratura, si è reso necessario uno studio preliminare riguardante l'espansione del letto di solidi granulari monodispersi e di miscele binarie di solidi con il fine di comparare i risultati ottenuti sperimentalmente con i risultati ottenuti dalle simulazioni numeriche. Per le simulazioni numeriche si ringrazia la collaborazione de l' *Institut de Mécanique des Fluides de Toulouse*.

Gli esperimenti sono stati condotti con due diverse granulometrie di *glass beads* appartenenti al gruppo B della classificazione di Geldart.

Si è calcolato teoricamente la velocità di minima fluidizzazione per i casi monodispersi e la si è confrontata con i risultati sperimentali ottenendo una buona corrispondenza.

In un tipico grafico rappresentante le perdite di carico in funzione della velocità superficiale del gas, la velocità di minima fluidizzazione è assunta come la velocità corrispondente al punto di intersezione tra la retta interpolante i valori di pressione misurati in condizioni di letto fisso e quella interpolante i dati relativi al letto

pienamente fluidizzato. Ulteriori incrementi della velocità superficiale del gas di fluidizzazione non comportano variazioni nella pressione media misurata.

Si è valutato il grado di vuoto, il quale assume un valore maggiore all'incrementare della velocità superficiale del gas.

L'espansione del letto è maggiore per il caso studiato di *coarse particles* rispetto al caso di *very coarse particles*.

I risultati ottenuti sperimentalmente sono in accordo con i risultati ottenuti dalle simulazioni numeriche.

In caso di fluidizzazione di miscele binarie la curva di fluidizzazione (perdite di carico in funzione della velocità superficiale) si modifica. La transizione da letto fisso a letto fluidizzato (regime dinamico) non si ha più per un valore unico, ben definito, di velocità. Il passaggio avviene gradualmente. Aumentando la velocità superficiale aumentano le perdite di carico, nella sequenza: letto fisso, regime statico ($U_{fi}<U<U_{fa}$), regime di transizione ($U_{fa}<U<U_{cf}$), regime dinamico ($U>U_{cf}$).

È possibile determinare sperimentalmente il valore di U_{cf} che risulta essere dipendente dalla percentuale di *coarse particles* presenti nella miscela.

Si sono effettuati degli esperimenti in discontinuo, i quali possono rivelarsi uno strumento utile nello studio dell'elutriazione, fenomeno che porta ad una condizione non stazionaria all'interno del reattore per via dell'allontanamento delle particelle più fini.

Il moto d'insieme del flusso di particelle è stato valutato conducendo degli esperimenti con le miscele e valutandone l'andamento dell'elutriazione delle particelle fini. Per valutare l'accuratezza degli esperimenti, per ogni miscela sono stati condotti due esperimenti. Al termine di ogni esperimento è stata recuperata e pesata la polvere che si trovava nella colonna di recupero. Per ogni esperimento è stato eseguito lo stesso protocollo.

Durante questa modalità batch è stato possibile determinare che la massa di solidi trascinati è stata sempre prossima al valore ipotizzato, valore massimo che è

possibile recuperare nota in ogni caso la percentuale di *coarse particles* nella miscela.

Nel caso di miscele i risultati ottenuti tramite gli esperimenti sono in accordo con i risultati ottenuti dalle simulazioni numeriche e dal comportamento ipotizzato dai dati di letteratura e dagli studi precedenti. Come anche dimostrano le simulazioni numeriche, il reattore presentava un elevato grado di mixing e non sono stati riscontrati apprezzabili fenomeni di segregazione.

Per valutare come la presenza di particelle di diametro maggiore influenzasse il moto d'insieme delle particelle più fini si è deciso di misurare la *Particle Size Distribution* delle particelle raccolte. Nella colonna di recupero si sono prelevati tre campioni a diverse altezze i quali successivamente sono stati analizzati.

Il particolare andamento della PSD riscontrato è probabilmente da attribuirsi alle distribuzioni granulometriche dei singoli casi monodispersi che per certi intervalli si sovrappongono.

L'ultima parte del lavoro è stata dedicata allo studio dei *Circulating Fluidized Bed.* Il fine era il raggiungimento di uno stato stazionario negli esperimenti di laboratorio, utilizzando un processo di ricircolo, il quale permette un confronto più agevole con i risultati ottenuti dalle simulazioni numeriche. La colonna di ricircolo, che permette alle polveri di tornare nella colonna primaria, è stata messa in funzione e ha dato buoni risultati. Non è stato possibile purtroppo tarare la sonda a microonde la quale permette di avere delle misurazioni in continuo nella testa del reattore. Non si hanno pertanto possibili comparazioni con dati di letteratura o con simulazioni numeriche.

In futuro si potrà studiare il comportamento fluidodinamico di diverse tipi di miscele formati da particelle di dimensioni diverse da quelle considerate in questo studio.

Investigare sul comportamento delle miscele sarà utile per progettare reattori più performanti e innovativi.

INDEX

Introduction

The aim of this study is the characterisation of the gas – solid hydrodynamic in the Fluidized Bed.

It has been necessary a preliminary study of bed's expansion of granular solids and binary mixtures of solids with the ultimate aim to be able to model the behavior in numerical simulations.

The Institute of Fluid Mechanics of Toulouse (IMFT) dealt the part of numerical simulations. To be able to compare the results of experiments and the results of numerical simulations it has been decided to use particles of group B according to Geldart's classification. The reason is because in previous studies is shown that bed expansion for Geldart A particles have a strong dependence on the mesh size used to compute the flow, leading to a major overestimation and powders of group C can hardly be fluidized since they channel easily in the bed and prevent good fluidization quality due to their strong interparticle adhesion forces, which greatly limit their application in various industrial processes although they often have so high a specific surface area that they are of particular advantage to chemical reaction processes. Therefore, the handling of these cohesive powders in the process of manufacturing catalysts, aerosols, plastics, metals, ceramics, foods and pharmaceuticals with fluidization has become increasingly important. It has turned into a worldwide effort to improve the fluidization quality of beds of cohesive powders.

1 CHAPTER ONE

THE HOST INSTITUTION AND THE DEPARTMENT

The host institution for which it has been possible to realize this work is the *National Polytechnic Institute of Toulouse* (also called INP Toulouse or INPT). Founded in 1969, is a French university system based in Toulouse, France part of University of Toulouse.

The Institute is composed of seven schools (six engineering schools and one school of veterinary medicine.) One of these is *École nationale supérieure des ingénieurs en arts chimiques et technologiques* (ENSIACET) where is situated the *Laboratory of Chemical Engineering.*

The *Laboratory of Chemical Engineering* (LGC), UMR 5503, which employs about 300 people (researchers and teachers, technical staff, PhD and Post Doc), is a CNRS research unit operated jointly by the CNRS, the Institut National Polytechnique of Toulouse (INPT) and the University - Paul Sabatier (UPS) of Toulouse. The research staff of the LGC is accommodated in four different buildings located in INP-ENSIACET, INP-ENSAT, UPS- Faculty of Engineering Science (FSI) and Faculty of Pharmaceutical Science (FSP).

The research is particularly active in the design of hybrid processes, microprocesses, processes for the production of advanced materials including micro or nanoparticles, nanostructured objects, the production of carbon-free energy, the treatment of water and waste water, and healthcare engineering. The Laboratory scientific approaches are both experimental and computational (modeling, simulation, optimization, design). The LGC has a series of pilot plants covering the laboratory scale up to the demonstrators in which real industrial conditions can be approached. The laboratory also develops specific experiments at the nano- and micro-scales generating fundamental data. It also benefits from a large pool of instruments for characterization and analysis (scanning electron microscopy, characterization of particles, chromatography, ICP, etc.) gathered in the Service for Analysis and Processes (SAP) on the INP-ENSIACET Campus or in the Measurements and

Analysis Service on the UPS-FSI campus. In addition to these experimental techniques specific means of calculation and commercial or internally developed software are available. The laboratory also trains through research , a large number of students (master, doctorate, post-doctorate) and maintains a regular partnership with socioeconomic partners for the transfer of new scientific knowledge and innovative technologies through training or research contracts.

Research departments

The LGC is composed of six scientific departments which are supported by technical and analytical services

Interface and Particle Interaction Engineering (GIMD)

- Study of the physical or physico-chemical interactions playing a role in solid-liquid, liquid-liquid or gas-liquid interfaces in dispersed phase or membrane processes . The generation and behavior of interfaces are studied by connecting mechanisms at a very small scale with the macroscopic properties of the medium and/or the process.

Electrochemical Processes (PE)

- Development of methods and electrochemical tools for the design, sizing and control of processes: phenomena and chemical reactions in real media using multi-scale experimental and numerical approaches by confronting the laws and concepts of physic-chemistry to real media.

Innovative Multiphase Reactor Engineering (IRPI)

- Development of new multiphase reactors with or without chemical reactions. Skills in catalytic reactor engineering, advanced oxidation, fluidization, CVD and activation are used for applications in environmental decontamination, energy and the development of new materials.

- *Bioprocesses and Microbial Systems* (BioSyM)

    - Understanding and driving microbial activity in agronomy and food industry processes, energy production, as well as environmental and healthcare sectors. Researchers from BioSyM bring together expertise in process engineering, industrial microbiology, physiology of microorganisms, bio-electrochemistry and toxicology.

- *Science and Technology of Intensified Processes* (STPI)

    - Design, scale-up, operation and security of intensified processes involving multifunctional instruments, green solvents, energy efficiency and biosourced carbon. Research focuses on industrial scale processes, associating equipment design and technology, as well as final product specifications.

- *Process System Engineering* (PSE)

    - Development of a systemic approach of innovative engineering and optimal operation of sustainable processes, from the molecule to the enterprise scale: generic tools for modeling, simulation, multi-objective optimization, to design interconnected equipment in a production unit.

- The research finds applications in the environment, energy, biology and health.
- The laboratory is involved in several networks and federations such as:
- Thematic Network of Advanced Research ("Sciences et Technologies pour l'Aéronautique et l'Espace")
- Water Competitiveness cluster
- FERMAT Federation ("Fluids, Energy, Reactions, Materials and Transfers")
- Rio Tinto Alcan-CNRS , a common team for molten-salt processes.
- Research-driven clusters:

    - AMC2 (Multi-physical Approaches for Colloids),
    - Bio-systems for engineering

2 CHAPTER TWO

PHENOMENOLOGY OF FLUIDIZATION GAS-SOLID

Fluidization is an unit operation through which a bed of granular solid buys typical properties of the fluids, obtained thanks to the passage of a fluid (gas) through the granular solid at a suitable speed. In the fixed bed the particles are in direct contact with each other, supporting each other's weight. When there is a large difference in the densities of the fluid and solid phases an increase in fluid velocity typically causes large bubbles or other such instabilities. Several types of instabilities are described by Kunii and Levenspeil. (1991).

Fluidized beds are used in different areas; examples are process of thermal conversion (combustion, gasification) of solid fuels (coal, biomass) and catalytic processes involving a gas and a solid catalyst (FCC). The fluidized bed is also used in the production of carbon nanotubes.

It is possible to summarize the advantages and disadvantages of fluidized beds.

Advantages

- Greatly improved bed-to-wall and bed-to-immersed surface heat transfer,
- Reduced axial and lateral temperature gradients, minimizing the probability of hot spots, catalyst sintering, and unwanted side reactions,
- Ability to add or remove particles continuously or intermittently, without shutting down the process,
- Reduced pressure drops (The pressure drop across the bed, once fluidized, essentially remains equal to only that required to support the weight of the bed.),
- Smaller catalyst particles, leading to improved catalyst effectiveness factors,
- Ability to introduce (usually as a spray) modest quantities of liquid reactants that vaporize before reacting or yield solid products upon reaction inside the bed.

Disadvantages

- Substantial axial gas mixing, causing much larger deviations from plug flow than for packed bed reactors, thereby adversely affecting conversions and selectivities,
- For reactions where the particles themselves react, substantial particle mixing, greatly broadening solid residence time distributions relative to moving beds,
- Particle attrition because of particles colliding with each other and with fixed surfaces,
- Wear on immersed tubes and other interior surfaces because of the particle impingement,
- Entrainment of particles, causing loss of catalyst and/or solid product, contributing to air pollution and requiring gas–solid separation equipment,
- Increased risk because of complex hydrodynamics and difficulties in characterizing and predicting reactor performance.

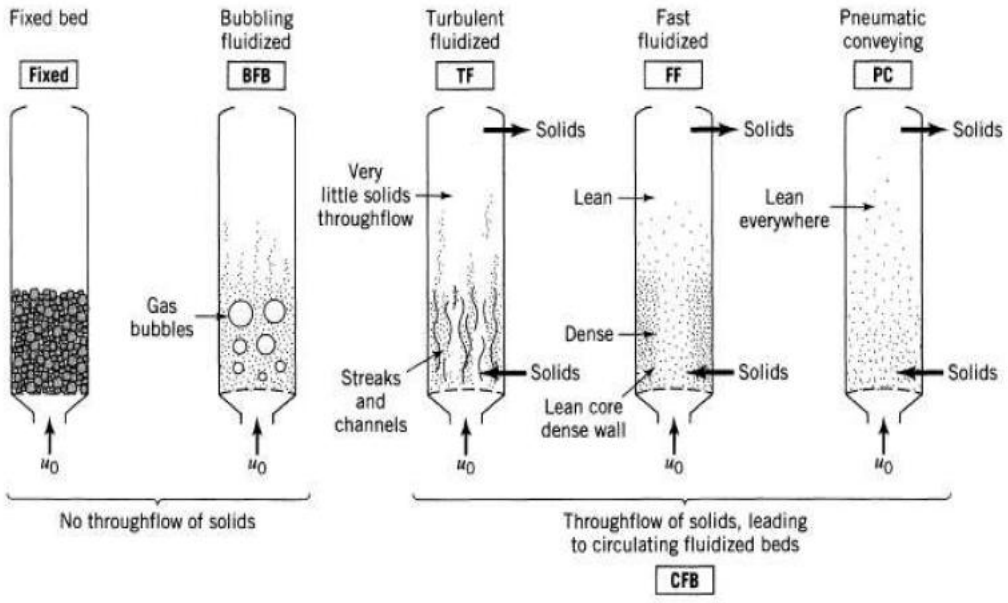

Figure 2.1 Different regimes of fluidization

It is possible to observe the transition from fixed bed to bubbling fluidized bed when increase superficial gas velocity.

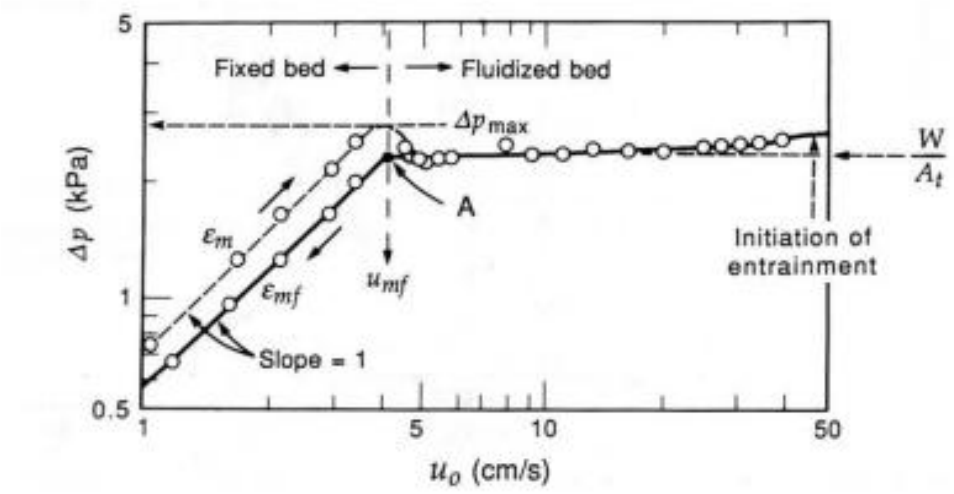

Figure 2.2 Transition from fixed bed to fluidized bed

At the beginning, for velocity less than velocity of minimum fluidization (U_{mf}), the bed behaves as a fixed bed, and gas pressure drop inside the bed are an increasing function of the superficial velocity, until velocity of minimum fluidization, after this U_{mf} gas pressure drop through the bed equals the weight of the bed per unit of section and remains constant and equal to the weight of the bed per unit of cross-section, particles begin to be incurred by the gas stream and it is possible to define the transition to fluidized bed.

Hydrodynamic behavior of gas–solid flow in the bubbling fluidized beds depends upon the particle properties. In a system consisting of particles of equal density, but different sizes, the bigger (heavier) particles tend to reside at the bottom of the bed.

The fluidization behavior of a binary mixture differing in particle sizes with the same density is strongly influenced by the variations of average particle diameter and mass fraction in the bed. The initial fluidization state of a binary mixture is characterized

by the minimum fluidization velocity at which the total pressure drop equals the particles weight per unit area of bed, which depends upon the averaged mass fraction of small particles. Therefore the fraction of small particles in the mixture is an important parameter of size segregating system.

2.1 Geldart's Classification

In order to identify the behavior of granular systems respect to fluidization, Geldart proposed an empirical classification through which it is possible assemble the powder into four classes.

Geldart (1973) observed the nature of particles fluidizing. He categorized his observations by particle diameter versus the relative density difference between the fluid phase and the solid particles.

He identified four regions in which the fluidization character can be distinctly defined.

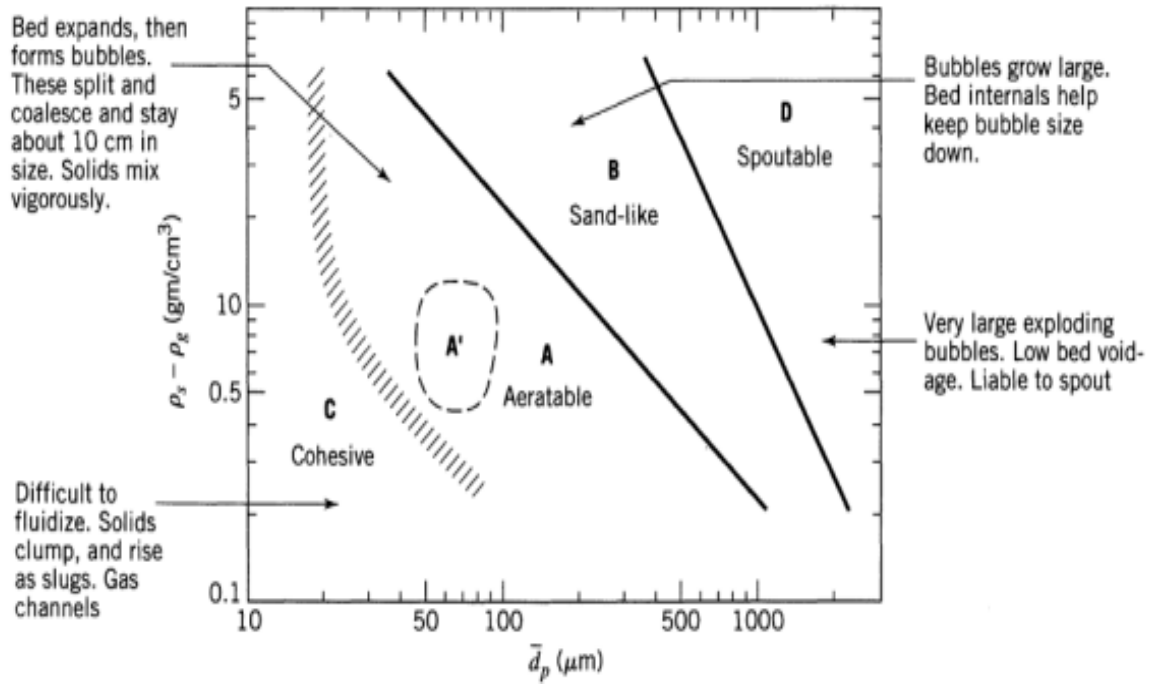

Figure 2.3 Classification of powder according to Geldart

Group A particles are characterized by

- Bubbling bed fluidization,
- The bed expands considerably before bubbling occurs,
  - ◊ Gas bubbles rise more rapidly than the rest of the gas,
  - ◊ Bubbles spit and coalesce frequently through the bed,
  - ◊ Maximum bubble size is less than 10 cm,
  - ◊ Internal flow deflectors do not improve fluidization,
- Gross circulation of solids occurs.

Group B particles. Beds of particles B are most common

- Are made of coarser particles than group A particles and more dense,
- Form bubbles as soon as the gas velocity exceeds U_{mf},
- Form small bubbles at the distributor which grow in size throughout the bed,
- Have bubble sizes independent of the particle size,
- Have gross circulation.

Group C particles

- Are difficult to fluidize and tend to rise as a slug of solids,
- Form channels in large beds with no fluidization,
- Tend to be cohesive.

Group D particles

- Are very large, dense particles,
- Form bubbles which coalesce rapidly and grow large,
- Form bubbles which rise slower than the rest of the gas phase,
- Form beds whose dense phase surrounding the bubbles has low void,
- Cause slugs to form in beds when the bubble size approaches the bed diameter,
- Spout from the top of the bed easily.

2.2 Elutriation

Elutriation is a process that fines are selectively carried out of the freeboard from a fluidized bed when the terminal settling velocity of small particles is lower than gas velocity. Whether the solids carrying out of the fluidized-bed reactor is a disadvantage or not in industrial processes, the elutriation rate needs to be estimated by designers in order to determine properly the freeboard and separators. The driving force in elutriation is the difference between gas velocity and free-fall terminal velocity of particle.

A first-order rate equation has been used to calculate the elutriation rate constant of fines from a fluidized bed by some investigators (Chang et al., 2005; Colakyan and Levenspiel, 1984; Li and Kato, 2001; Wen and Chen, 1982). The elutriation rate constant can be expressed by operating parameters, e.g., superficial gas velocity, fine particle size and properties of solids and gas.

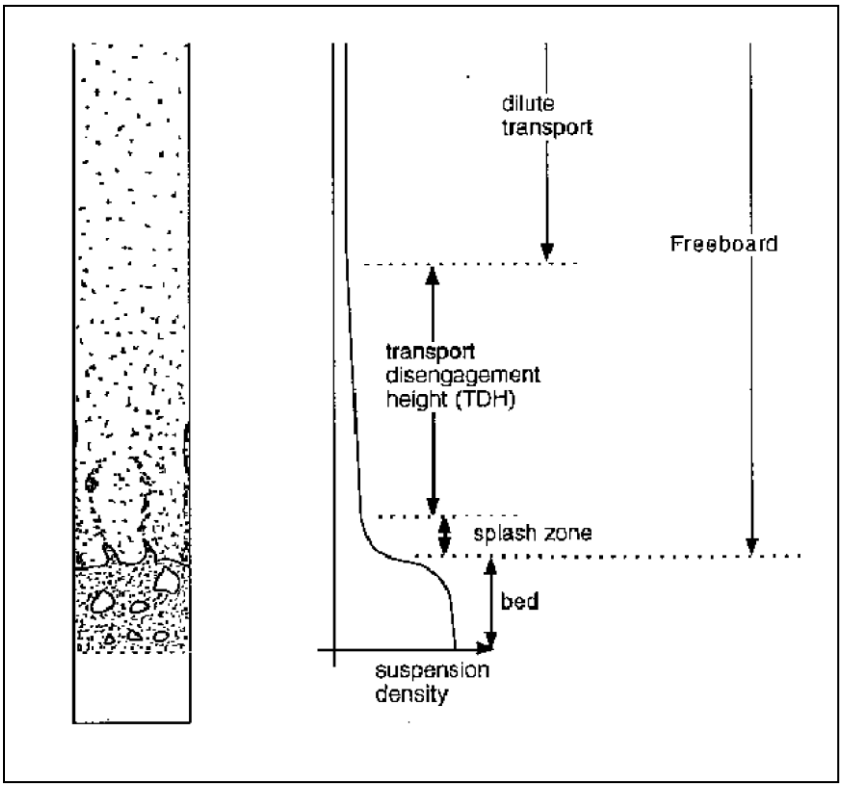

Figura 2.4 Phenomenology of elutriation

In bubbling fluidized bed combustion and catalytic cracking, elutriation is a major cause of inefficiency, it is possible to lose a part of reactant or a product and affect the economy of the process, while it is highly desirable, for instance, in sludge incineration. Whether the intention is to quench or promote elutriation, the involved phenomena must be properly identified if the process is to be efficiently controlled, so it's necessary to be able to estimate elutriation rate to design properly reactors, cyclones and separators.

Table 2.1 Published correlations for the elutriation rate constant

Table 2
Published correlations for the elutriation rate constant

Investigators	$d_{p,\text{coarse}}$ (μm)	$d_{p,\text{fine}}$ (μm)	Geldart group	U_o (m/s)	Correlation
Zenz and Weil (1958) [19]		20–150	A	0.30–0.72	$\begin{cases} \frac{K_i}{\rho_g U_o} = 125.5\times10^5\left(\frac{U_o^2}{gd_{pi}\rho_p^2}\right)^{1.87}, & \frac{U_o^2}{gd_{pi}\rho_p^2} \le 3.63\times10^{-2} \\ \frac{K_i}{\rho_g U_o} = 4.15\times10^4\left(\frac{U_o^2}{gd_{pi}\rho_p^2}\right)^{1.45}, & \frac{U_o^2}{gd_{pi}\rho_p^2} \ge 3.63\times10^{-2} \end{cases}$
Tanaka et al. (1972) [20]	141–2300	60–800	A/B	1.28–2.70	$\frac{K_i}{\rho_g(U_o-U_t)} = 0.046\left(\frac{(U_o-U_t)^2}{gd_{pi}}\right)^{0.5} Re_t^{0.3}\left(\frac{\rho_p-\rho_g}{\rho_g}\right)^{0.15}$
Merrick and Highley (1974) [41]	< 1400	1400–3170	A/B	0.61–2.44	$\frac{K_i}{\rho_g U_o} = A + 130\exp\left[-10.4\left(\frac{U_t}{U_o}\right)^{0.5}\left(\frac{U_{mf}}{U_o-U_{mf}}\right)^{0.25}\right]$ where $A = 10^{-4}$–1.5×10^{-3}
Geldart et al. (1979) [21]	150–355	38–327	A/B	0.60–3.00	$\frac{K_i}{\rho_p U_o} = 23.7\exp\left(-5.4\frac{U_t}{U_o}\right)^a$
Wen and Chen (1982) [24]			A/B		$K_i = \rho_p(1-\epsilon_t)(U_o-U_t)$ where $\begin{cases} \epsilon_t = \left(1+\frac{\lambda(U_o-U_t)^2}{2gD}\right)^{-1/4.7} \\ \frac{\lambda\rho_p}{d_p^2}\left(\frac{\mu}{\rho_g}\right)^{2.8} = \begin{cases} 5.17Re_t^{1.8}D^2, & Re_t \le 2.38/D \\ 12.3Re_t^{2.8}D, & Re_t \ge 2.38/D \end{cases} \end{cases}$
Colakyan and Levenspeil (1984) [25]	300–1000	36–542	A/B	0.901–3.66	$K_i = 0.011\rho_p\left(1-\frac{U_t}{U_o}\right)^2$
Kuto et al. (1987) [26]	58–252	37–150	A/B	0.2–1.1	$\frac{K_i}{\rho_p(U_o-U_t)} = 2.07\times10^{-1}\left(\frac{(U_o-U_t)^2}{gd_{pi}}\right)^n Re_t^{1.6}\left(\frac{\rho_p-\rho_g}{\rho_g}\right)^{0.61}$ $n = Re_t^{-0.4}$ (for Geldart group A particles)
Bueyens et al. (1992) [31]	30–77.8	10.1–13.9	A/C	0.2–0.7	$K = 5.4\times10^{-5}\rho_p\left(\frac{U_o}{0.2}\right)^{4.4}\left(1-\frac{U_t}{U_o}\right)^2$ (for $d_t < d_{t,\text{crit}}$)

[a] Modified from the original paper by using ρ_g in place of ρ_p.

The early work of Zenz and Well (1958) introduced two different theoretical approaches to describe the entrainment of solid particles throughout the freeboard of fluidized beds. According to the dynamic approximation, bubbles burst throwing particles which are subjected to inertia, gravitational and drag forces. Some sizes are carried up continuously and some only to certain heights, from where they fall back.

For sufficiently high freeboards, the particles carried away should have terminal velocities lower than the gas superficial velocity, while the falling particles should have terminal velocities higher than that. Entrainment is treated as a particle dynamic process, where momentum exchanges and trajectories of particles are among the relevant features to describe.

A considerable number of empirical correlations are available in the literature for predicting entrainment from fluidized beds, which are based either on dynamic or pneumatic views of the freeboard phenomena.

Nevertheless, among the available correlations, those developed by Merrick and Highley (1974) and Wen and Chen (1982) were validated for relatively large fluidized beds, and are reasonably well accepted.

As already shown, several observations by many authors have made it clear that the freeboard hydrodynamics is defined basically by: a gas stream carrying dispersed solids upwards; agglomerates of particles flowing upwards; agglomerates of particles flowing downwards. In summary, it has been shown that the present degree of knowledge of the freeboard phenomena is not enough to allow a reliable comprehensive modeling of elutriation, and the empirical correlations are not general or accurate.

2.3 Physical definitions

The minimum superficial velocity and the degree of void, defined as the volume fraction occupied by single fluid phase, in correspondence of which is manifested fluidization, characteristic for each specific gas-solid system, are define respectively the minimum fluidization velocity (U_{mf}) and void ratio (ε).

Equations used in this work to obtain minimum fluidization velocity, void ratio and terminal settling velocity are those widely employed in previous studies conducted and validated.

Archimede Number

$$Ga = \frac{{d_p}^3 * (\rho_p - \rho_g) * g}{\mu^2} \quad (1)$$

Reynolds Number

$$Re = [(31.6)^2 + 0.045 * Ga]^{0.5} - 31.6 \quad (2)$$

Thonglimp's Correlation

$$\varepsilon = 1.57 * Re^{0.29} * Ga^{-0.19} \quad (3)$$

$$\varepsilon = 1 - \alpha_p \quad (4)$$

$$Umf = \frac{Re * \mu}{d_p * \rho_g} \quad (5)$$

Wen and Yu Correlation, to determine the terminal settling velocity

$$C_{d,WY} = \frac{24}{Re_p}\left(1 + 0.15 Re_p^{0.687}\right) \alpha_g^{-1.7} \quad Re_p < 1000 \quad (6)$$

3 CHAPTER THREE

EQUIPMENT AND INSTRUMENTS

The experiments have been carried out in the laboratories of National Polytechnic Institute of Toulouse, in the Laboratory of Chemical Engineering.

The mock up consists in a primary column, steel made, of total height of 332.98 cm and internal diameter of 10 cm. In the top of this column there are the inlet of the powder and the microwave sensor (for a continuous measurement in time), while in the bottom there are the gas distributor and the inlet of primary air.

Figure 3.1 Mock up in laboratory

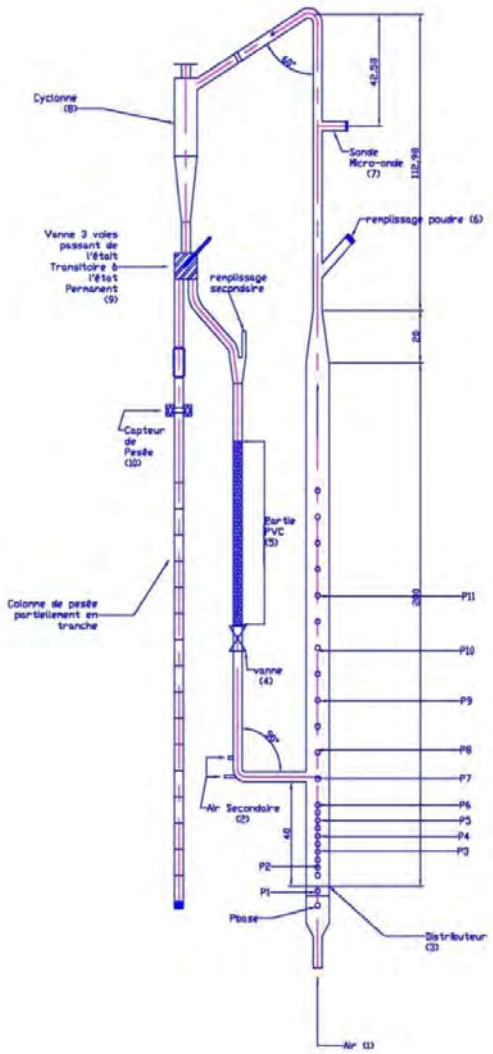

Figure 3.2 Scheme of the mock up

The gas distributor consists in a perforated plate (holes of 2mm diameter).

Figure 3.3 Perforated plate distributor

In the first part of the column we can measure the variation of pressure through 10 pressure sensors. The reference sensor, which gives the difference in pressure with each sensor, is placed at 151 cm, on top of all the others.

Table 3.1 Position of pressure sensor

Sensor	Position
P1	0 cm
P2	7.5 cm
P3	10.5 cm
P4	16.5 cm
P5	19.5 cm
P6	25.5 cm
P7	28.5 cm
P8	31.5 cm
P9	36.5 cm
P10	81.5 cm

After the cyclone, which recovers the particles entrained, we have two different columns. One is, polycarbonate made, having an internal diameter of 3.8 cm, it is characterized by the presence of one force sensor. This column is responsible to recover the entrained particles, to weigh them and perform some sampling to measure the PSD of these particles.

The second column, steel and polyvinylchloride made, is able to put off particles entrained in primary column through an injection of secondary air. This allows to have a continuous process and to work in recirculation.

3.1 Data measurement and acquisition unit

Since the project aims to carry out the diagnostic of the dynamics regime in the reactor based on pressure measurements, it has been necessary to set up an adequate data logging system.
The pressure measured is transferred in the form of electrical signal.

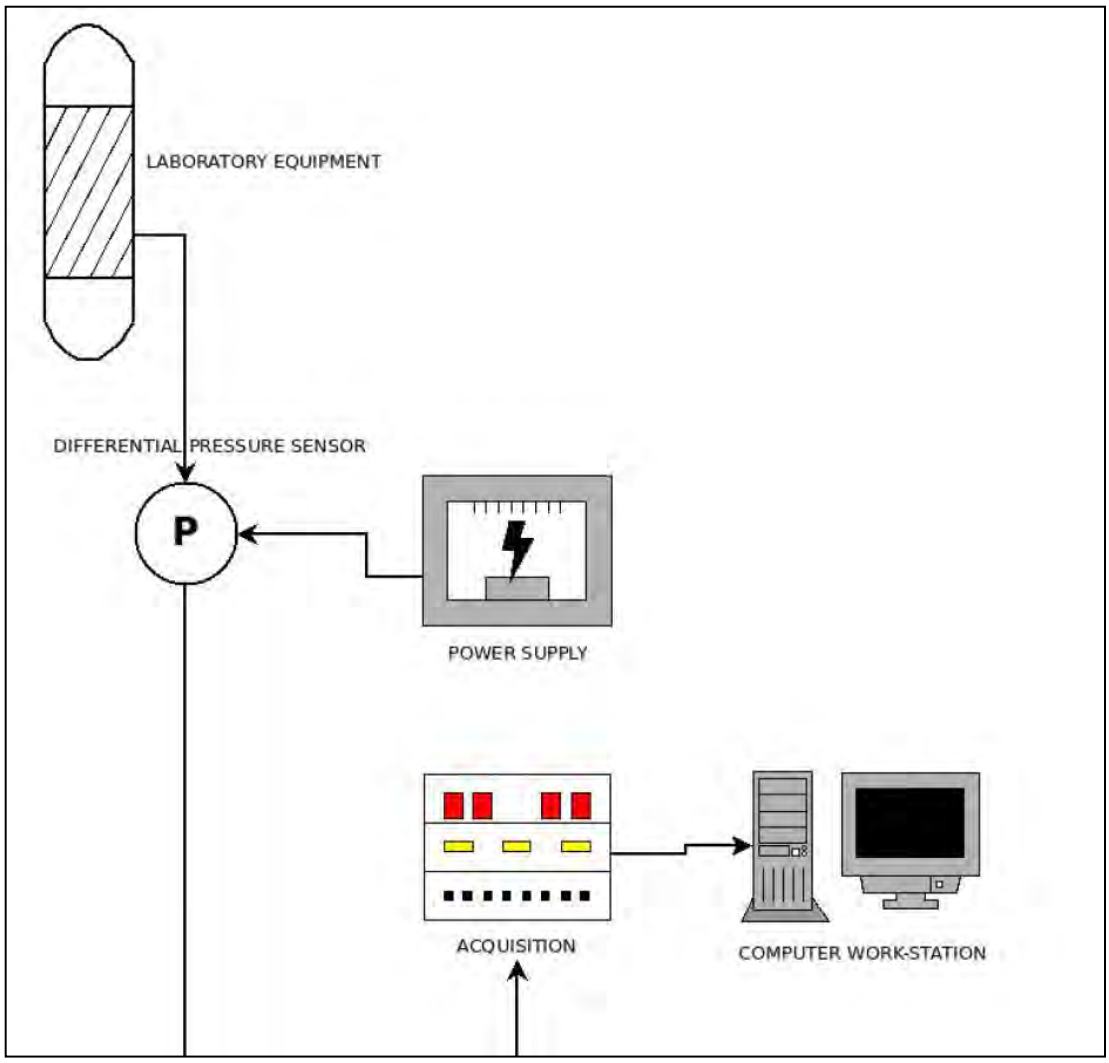

Figure 3.4 Data measurement and acquisition unit

In Fig. 3.4 the data acquisition unit is shown, connected to a computer. It allows a direct monitoring of the electrical signal during time and thus the control of the pressure fluctuations inside the reactor.

4 CHAPTER FOUR

HYDRODYNAMIC STUDY OF MONO-DISPERSE POWDERS IN FLUIDIZED BED

This chapter describes the operating conditions and the properties of the materials used for the experiments. We also exposed granulometric analysis for the two different particle sizes. Finally, results are presented for the mono-dispersed cases of the expansion of the bed and the comparison with the results obtained through numerical simulations.

4.1 Operating conditions

The experiments have been conducted at atmospheric pressure (P = 1 atm) and at temperature of 16°C (T = 16°C) without chemical reaction.

4.2 Material properties

The powders used in the experiment are glass beads of two different sizes belonging to Group B in Geldart's classification. To avoid electrostatic forces particles have been treated with a mixture of water and detergent for two hours. Subsequently, the water has been removed and particles put in a oven for four days at T = 45°C.

To determine material's characteristics, such as size and density, we used a Mastersizer 2000, with a pressure of dispersion of 2.5 bar, for granulometric analysis and a helium pycnometer to determine the intrinsic density.

Granulometric analysis allows the analysis of suspensions and emulsions with a particle size in the range 0.02/200 micrometres. This instrument uses the technique of laser diffraction (low angle laser light scattering) which provides information about the size of the particle, starting from the analysis of the radiation scattered by a particle hit by a monochromatic radiation.

The measurement of bulk density has been achieved by helium pychnometry. This technique is based on measurement of the weight of the solid and the volume of the tank not occupied by solid.

Table 4.1 Materials' properties

Materials - Glass Beads	**Coarse particles**	**Very coarse particles**
Particle size range (μm)	170 - 360	346 - 735
Sauter mean diameter d[3,2] (μm)	237.725	484.610
Density (g/cm^3)	2.4835	2.4918
Archimede's Number	1219.723	10332.700
Reynolds' Number	0.809	6.317
Geldart Classification	B	B
Minimum fluidization velocity by Thonglimp correlation (m/s)	0.051	0.195
Terminal settling velocity by Wen and Yu correlation (m/s)	1.78	4.18

Although the density and the Geldart Classification are the same, due to the different particle size range we can distinguish that the Archimede's Number for larger particles is almost 10 times the value of smaller. The Sauter mean diameter for very coarse particles is 2 times of coarse particles, this influence the Reynolds' Number, the estimation of minimum fluidization velocity and terminal settling velocity from correlation. Both distributions are symmetric with respect to the maximum.

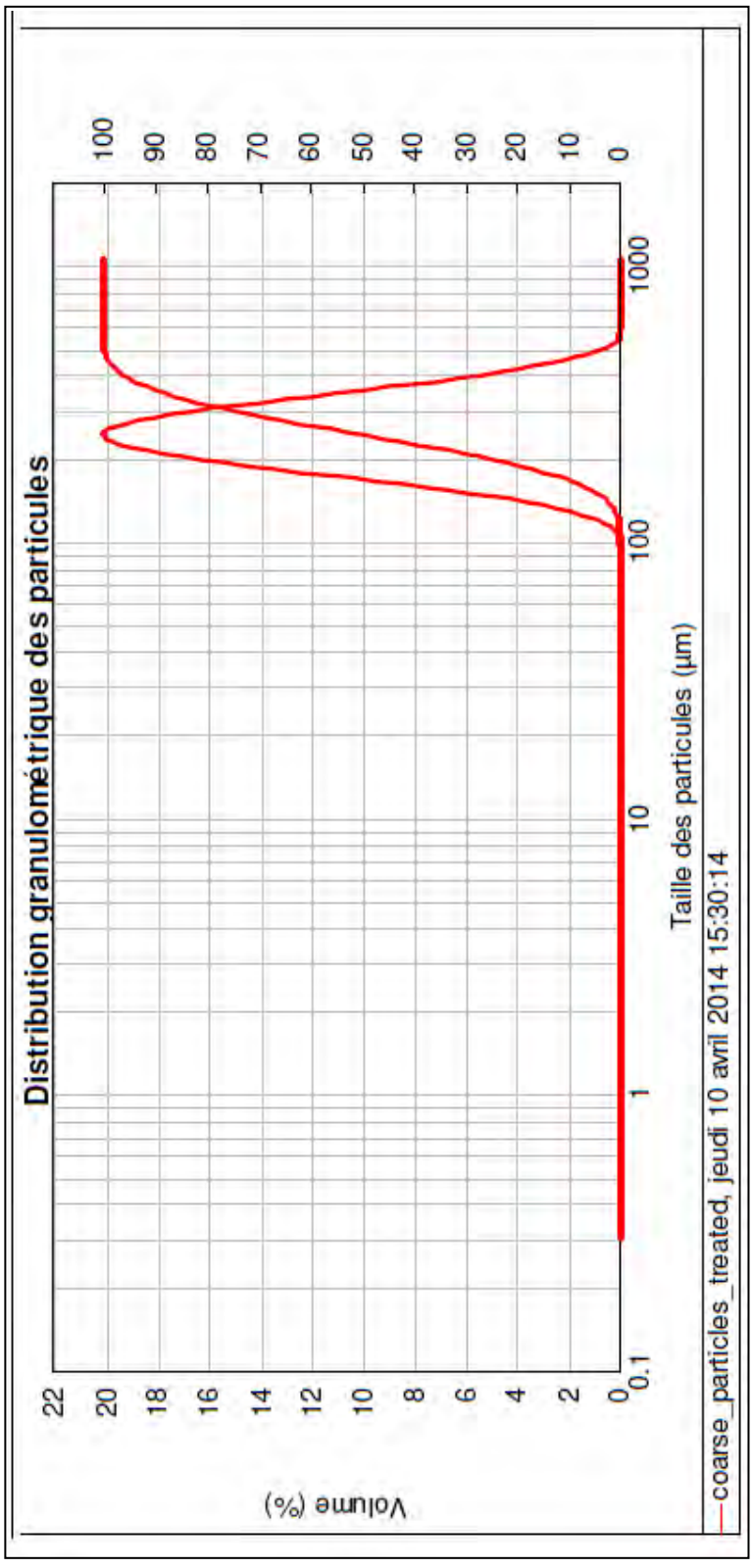

Figure 4.1 Particle Size Distribution of coarse particles

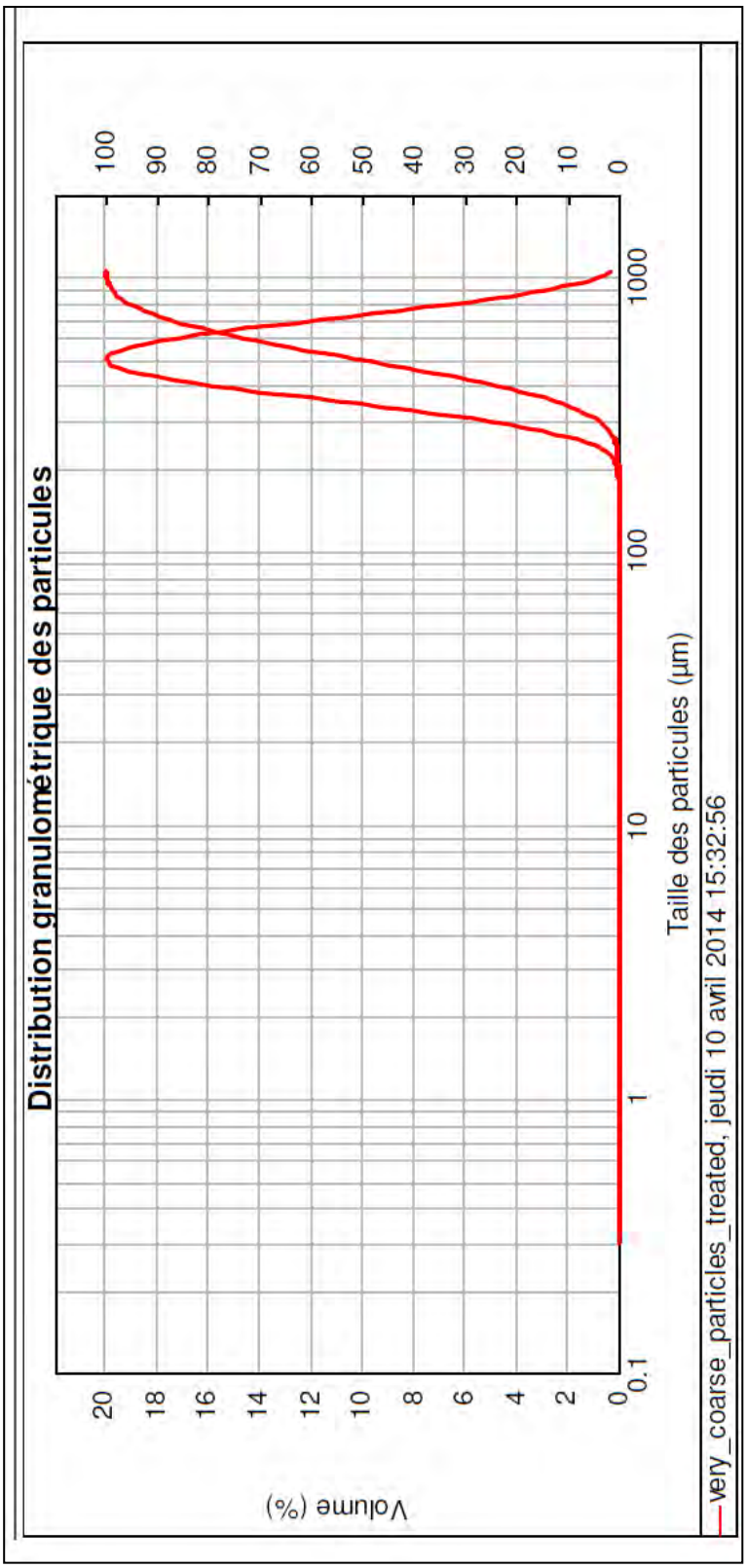

Figure 4.2 Particle Size Distribution of very coarse particles

The experimental campaign includes series of measurements of the bed pressure drop at different heights, from which the bed height can be estimated. Measurements cover a wide range of fluidization velocities, from the fixed state to the maximum perceivable degree of expansion.

The first step in this work has been the study of the expansion of mono-disperse dense fluidized bed.

It is recommended to use appropriate optimal velocity: $U = 1.5 \div 10 * U_{mf.}$ We always used a mass of 2.5 kg of glass beads. All experiments have been repeated 3 times to obtain a good reproducibility. The arithmetic mean, evaluated on the 3 trials, gives the value of pressure reported in the following figure.

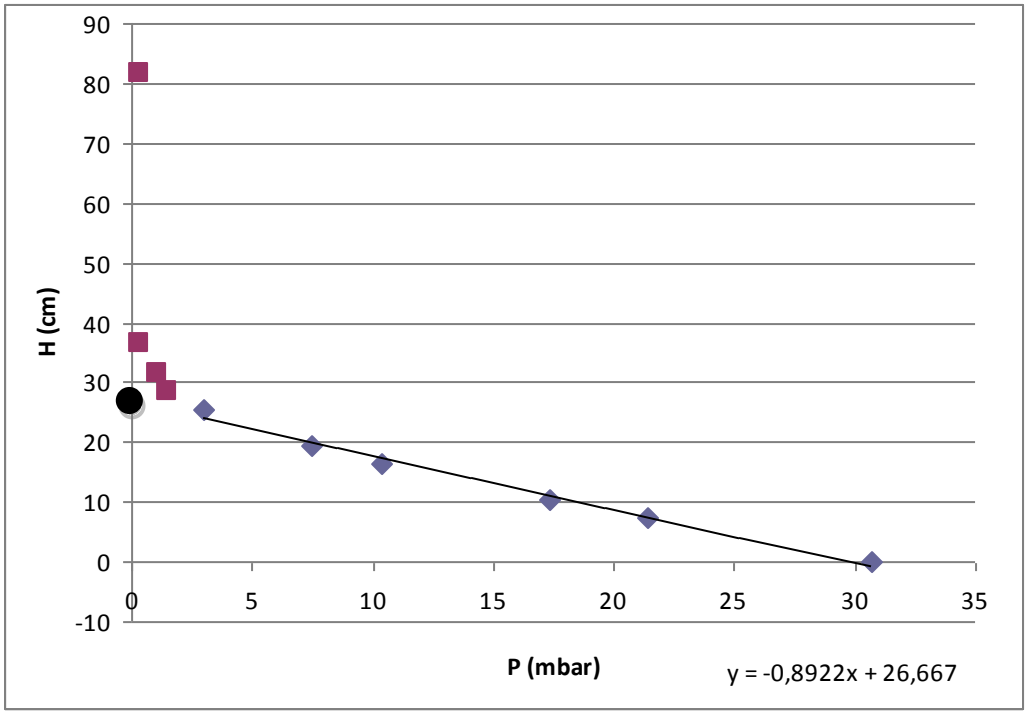

Figure 4.3 Height of the bed in mono-disperse case of coarse particles

For each experience a long fluidization period (seven minutes) has been considered. The fluidization of particles is the result of a balance between hydrodynamic forces and gravitational forces.

It has been possible to determine the height of the bed and the gas pressure drop per unit length by theory. The results agree with literature data found in the article of Girimonte R. and Vivacqua V. (2011).

To quantify the height of the bed and gas pressure drop per unit length a linear fit through the first 6 internal pressure sensor in the bed has been used.

$$\frac{dP}{dz} = (\rho_p - \rho_g) * g * \alpha_p \qquad (7)$$

The intercept of the line determines the height of the expanded bed. The height of the bed increases with increasing superficial gas velocity.

The gas pressure drop decreases with increasing superficial gas velocity.

It is possible to define a fluidization index, to describe the quality of fluidization, defined as the ratio of the pressure drop over the bed to the weight of the bed per unit cross-sectional area.

$$Quality\ Index\ of\ Fluidization = P1/(\frac{W}{A}) \qquad (8)$$

Table 4.2 Quality Index of Fluidization

	P1 [mbar]	(W/A) = Theoretical maximum pressure (Pmax_theo) [mbar]	P1/Pmax_theo
100% coarse particles at 0.485 m/s	30.725	31.242	0.983
100% coarse particles at 0.945 m/s	29.570	31.242	0.946
100% very coarse particles at 0.486 m/s	30.649	31.242	0.981
100% very coarse particles at 0.975 m/s	30.382	31.242	0.972

This value is always close to one, which allows us to consider each time a good degree of fluidization.

The value of minimum fluidization velocity has been determine experimentally. The velocity of minimum fluidization is assumed as the velocity corresponding to the point of intersection between the straight line interpolating the pressure values measured under the condition of fixed bed and the interpolating data relating to the fully fluidized bed.

The value of U_{mf} is close to the value calculated from Thonglimp's correlation.

Table 4.3 Comparison between theoretical and experimental U_{mf}

	Theoretical	Experimental
U_{mf} coarse particles (m/s)	0.051	0.053
U_{mf} very coarse particles (m/s)	0.195	0.19

Experimental data about U_{mf} are in agreement with the prediction of correlation. In the figure 4.4 is possible to distinguish the different expansion of the bed between the two different sizes of particles.

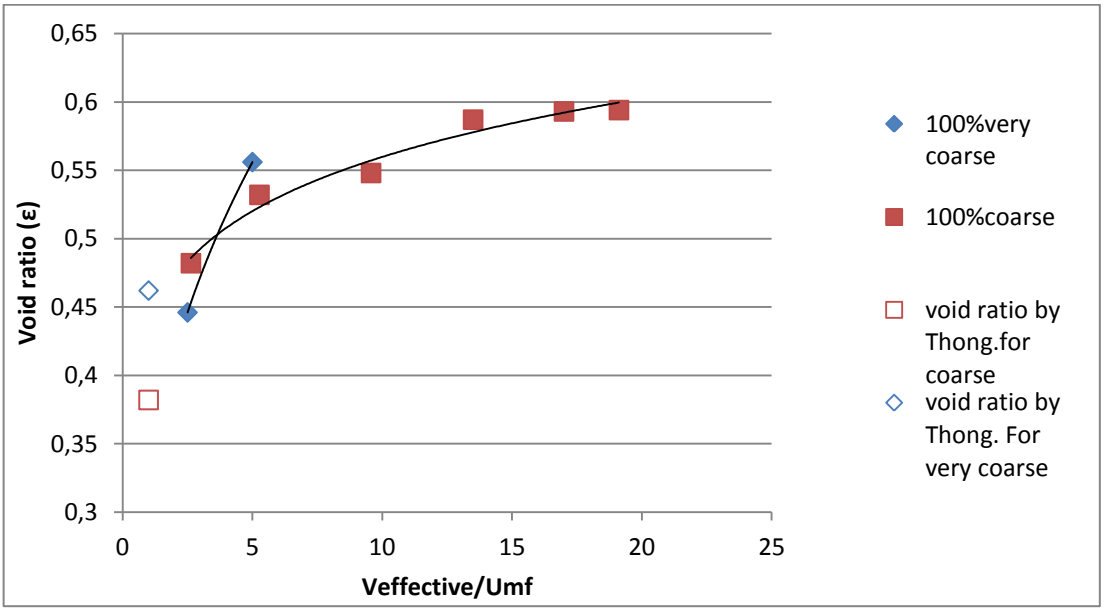

Figure 4.4 Void ratio in two different mono-disperse case

In the figure 4.4 we can recognize the different behavior between the different particles. The bed expansion for finer particles is higher than larger particles, as data literature argue. The void ratio found for smaller particles are in agreement with the behavior predicted by Thonglimp's correlation , differently results found for larger particles do not seem to agree with the theory.

Comparison between experimental data in two different mono-disperse case (100% coarse particles and 100% very coarse particles) and results obtained from numerical simulations are shown in Figure 4.5 and Figure 4.6.

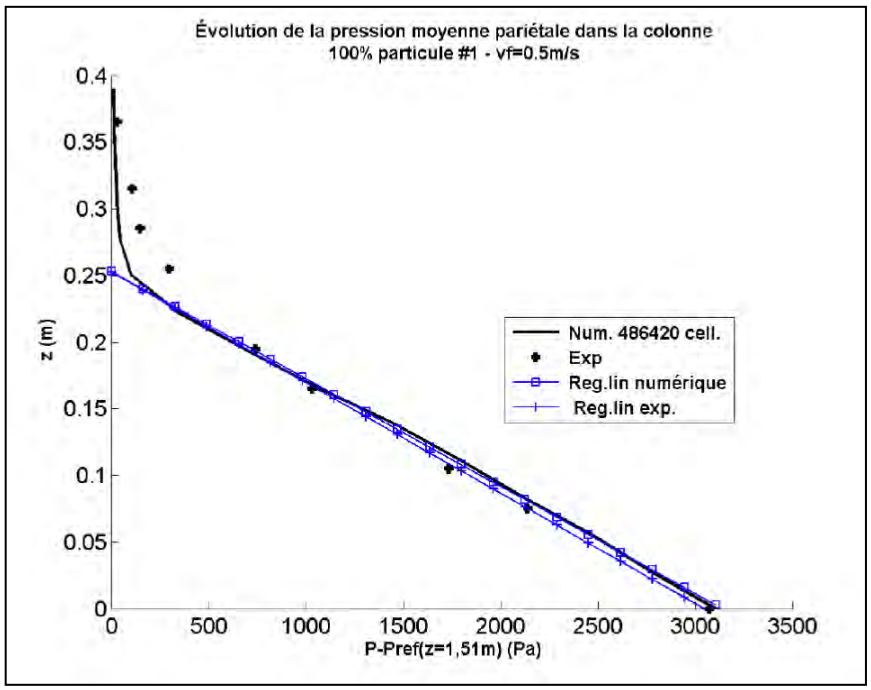

Figure 4.5 Comparison between experimental data and results obtained from numerical simulations of 100% coarse particles

The Institute of Fluid Mechanics of Toulouse has developed a code for the numerical simulations. The code Neptune_CFD process an Eulerian multi-fluid approach.

The model predicts reasonably the experimental data. As regards the mono-disperse case of coarse particles, the performance achieved by the simulation is found to be in

agreement with the behavior of the particles within the bed obtained by experiments. The prediction turns out to be less accurate in the freeboard.

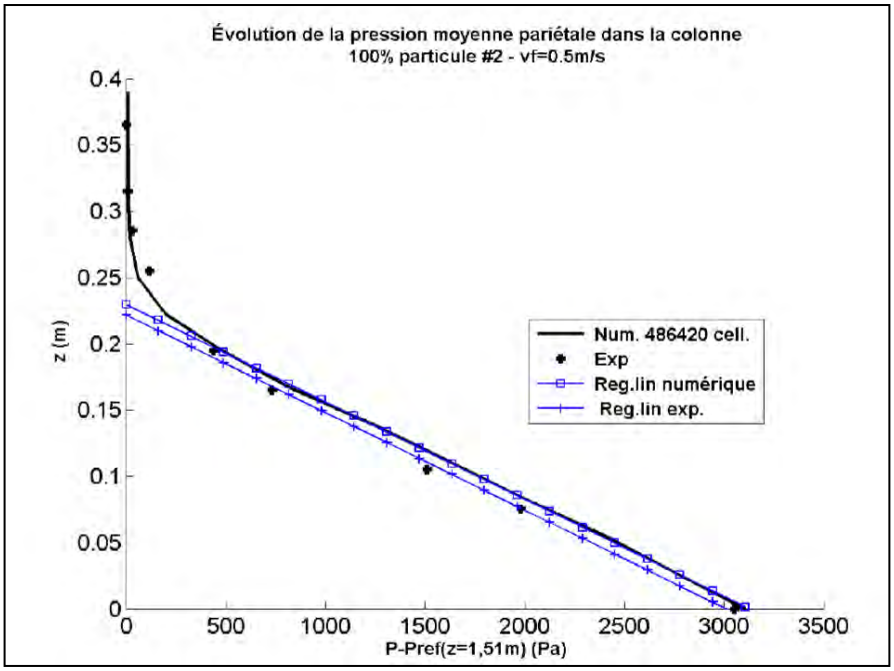

Figure 4.6 Comparison between experimental data and results obtained from numerical simulations of 100% very coarse particles

In the mono-disperse case of very coarse particles model turns out to be less predictive and the values obtained from the simulations are further removed the case mono-dispersed previously observed. However, the behavior in the freeboard is measured almost in the same way through experimental data and numerical simulations.

5 CHAPTER FIVE

HYDRODYNAMIC STUDY OF POLY-DISPERSE POWDERS IN FLUIDIZED BED

This chapter describes the experiments conducted using binary mixtures. We expose the results obtained about the gas pressure drop and the bed expansion. Finally, the comparisons with the results obtained through numerical simulations and experimental data for the poly-disperse cases are presented.

The following experiments have been conducted working with binary mixtures of glass beads. Total weight of mass solids is each time 2.5 kg.

The table below summarizes the characteristics of the mixtures employed.

Table 5.1 Material properties in mixture

Coarse particles		Very coarse particles	
d[3,2] = 237.725 μm		d[3,2] = 484.610 μm	
75%	1.875 kg	25%	0.625 kg
50%	1.250 kg	50%	1.250 kg
25%	0.625 kg	75%	1.875 kg

Each experiment has been repeated three times to ensure a good reproducibility. After a short period to ensure a good mixing of the two different classes of particles,

the binary mixture has been fluidized for a long period (seven minutes). For each value of gas pressure drop, the height of the bed and the void ratio have been determined as average of the three replicated experiments. The purpose of these experiments was quantifying the influence of larger particles in bed expansion.

In the following graph the trend of the pressure measured by the sensors in five cases has been reported.

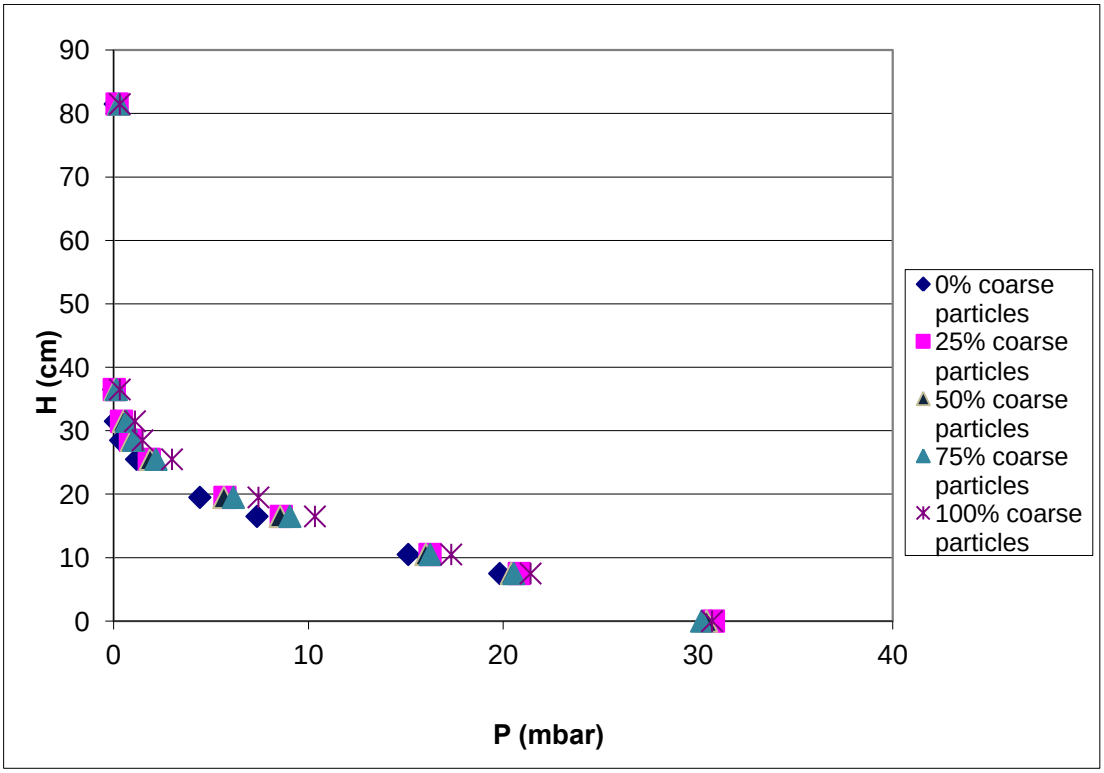

Figure 5.1 Pressure trend in five different cases

The pressure sensors, present in the reactor within the expanded bed, record different values at the same height after changing the percentage of fine particles present in the mixture. The values of pressure prove to be nearly identical when evaluated in the freeboard or just above the distributor.

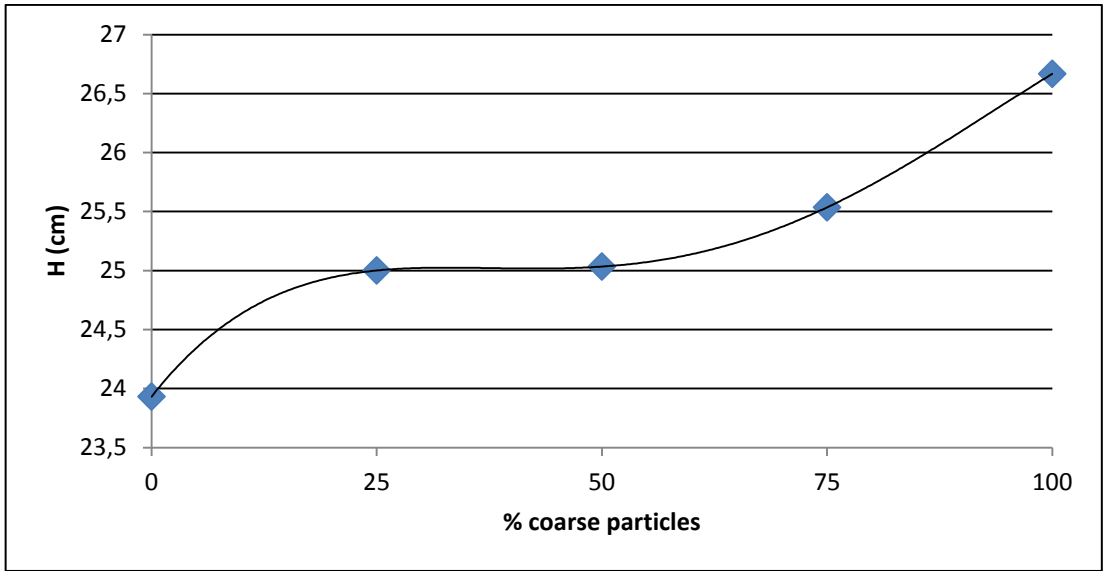

Figure 5.2 Height of the expanded bed in binary mixtures

The height of the bed increases with increasing the percentage of finer particles. However, the variation is not significant in the intermediate mixtures, between 25% and 50%.

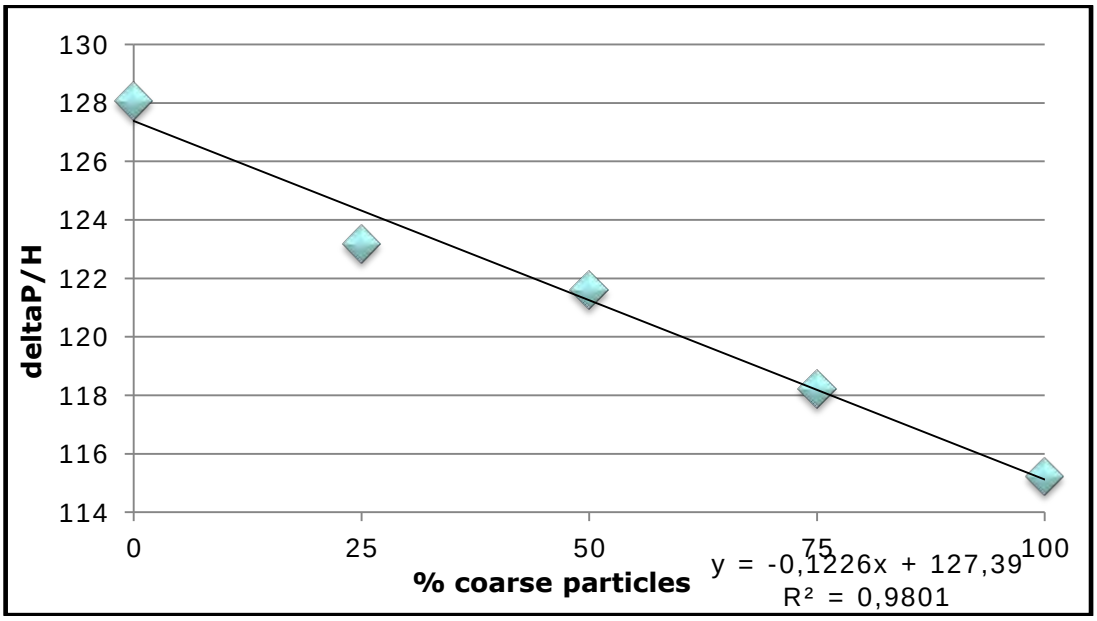

Figure 5.3 Gas pressure drop in five cases of binary mixtures

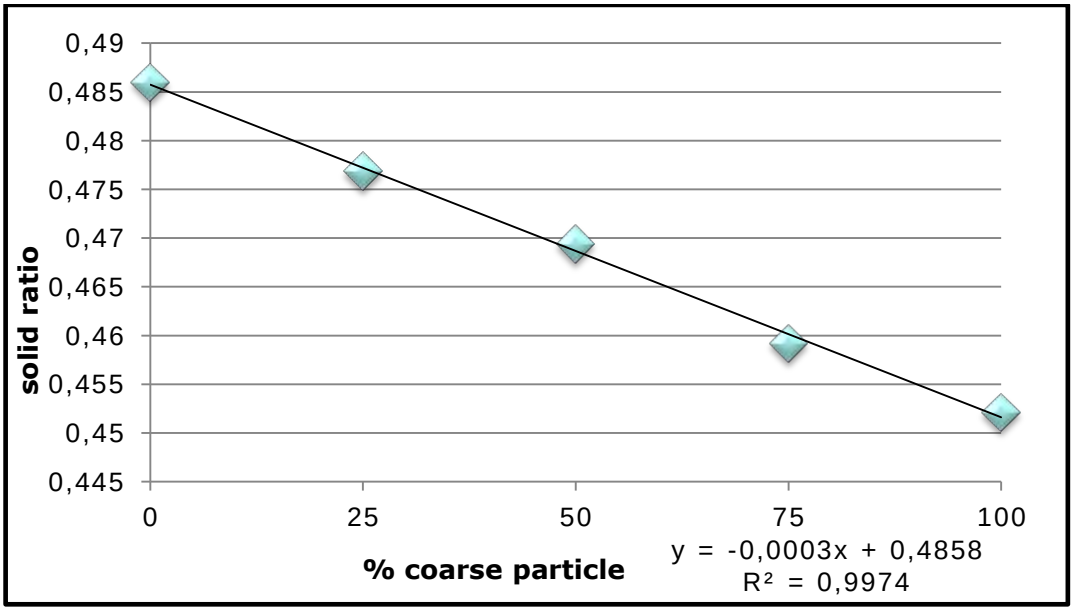

Figure 5.4 Solid ratio in binary mixtures

We can recognize inside the bed a linear behavior in the changing of gas pressure drop and solid ratio (volume fraction of solids) as a function of the percentage of coarse particles. Gas pressure drop decreases with increasing the percentage of smaller particles, while void ratio increases with increasing the percentage of smaller particles, consistent with intuition and data obtained from previous studies by Girimonte R. and Vivacqua V. (2011).

Table 5.2 Gas pressure drop and solid ratio

% Coarse particles	$\delta P/H$ (mbar/m)	α_p
0	128.065	0.485
25	123.172	0.476
50	121.606	0.469
75	118.210	0.459
100	115.217	0.452

Comparisons between experimental data and results obtained from numerical simulations, developed through Neptune_CFD code, in case of studies of three mixtures with different percentage of coarse particles are shown in Figure 5.5, Figure 5.6 and Figure 5.7.

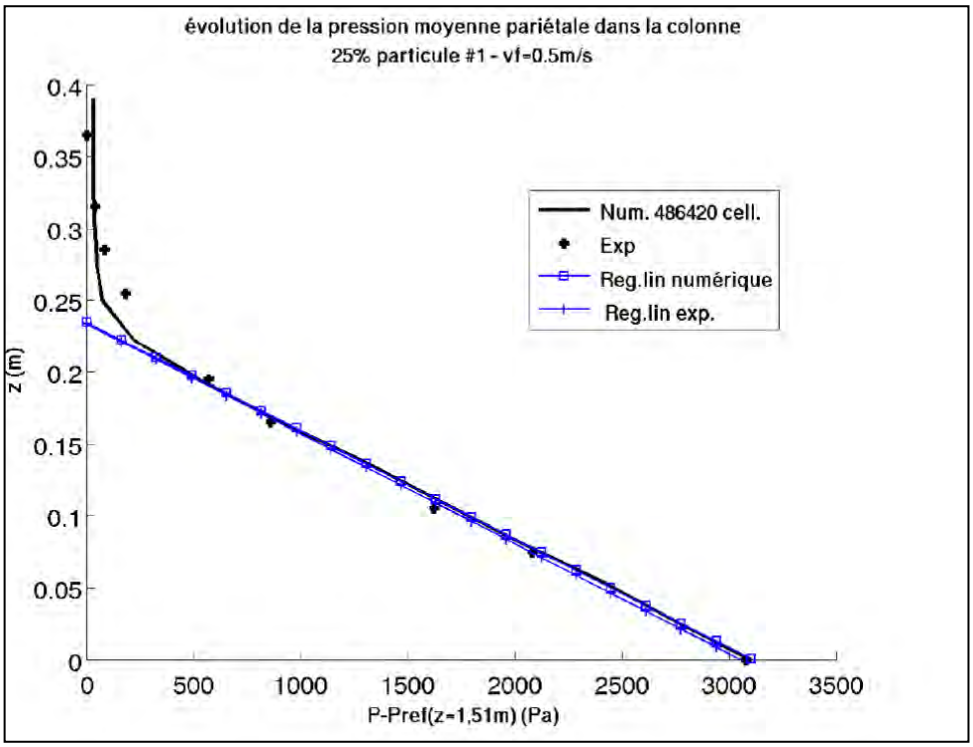

Figure 5.5 Comparison between experimental data and results obtained from numerical simulations of 25% coarse particles

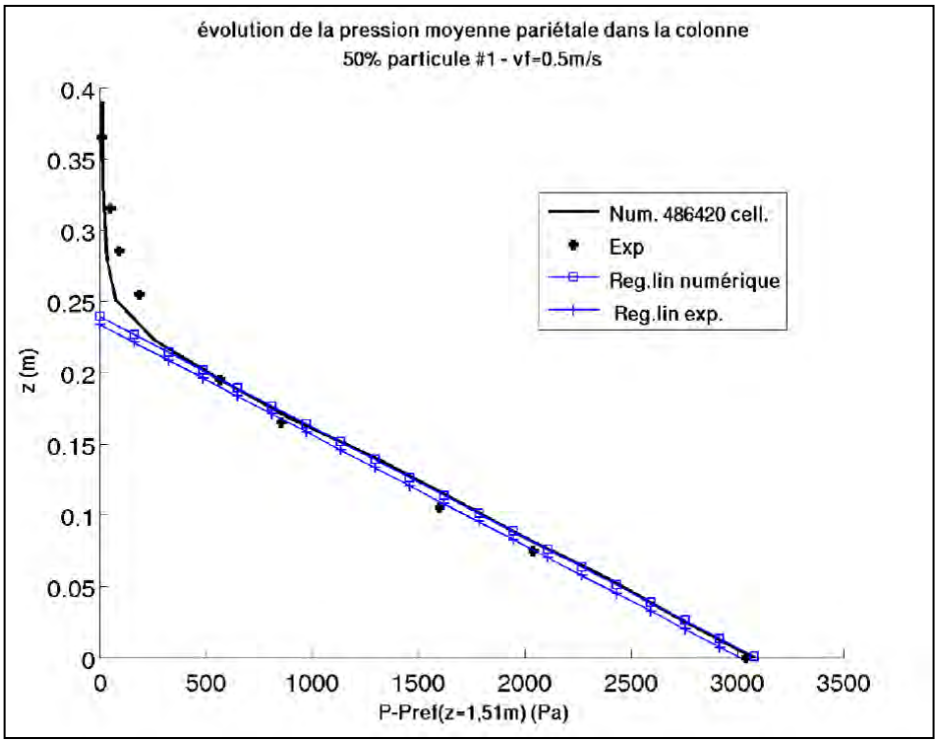

Figure 5.6 Comparison between experimental data and results obtained from numerical simulations of 50% coarse particles

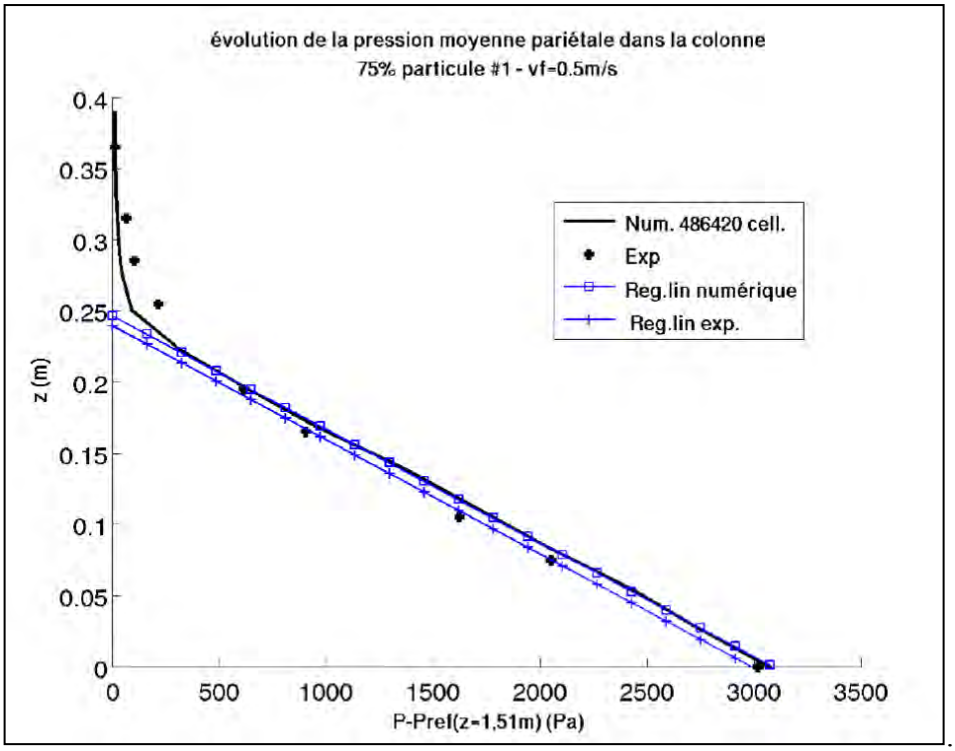

Figure 5.7 Comparison between experimental data and results obtained from numerical simulations of 75% coarse particles

In poly-disperse case, each time, the modeling predicts a pressure drop in the reactor very close to the data obtained experimentally. The height of the expanded bed obtained through numerical simulations has each time almost the same value than height obtained from experiments. We can recognize as the limits of the model the difficulties in modeling the behavior of the powders in the freeboard.

6 CHAPTER SIX

DIFFERENT REGIMES OF FLUIDIZATION IN A BINARY MIXTURE

In this chapter introduces the different fluidization regimes that occur in a binary mixture, given that the transition from fixed bed to fluidized bed is so sharp. It is shown how to determine experimentally the complete fluidization velocity (U_{cf}), which is important to understand the transition to fully fluidized bed. Finally, experiments conducted in a batch mode are presented, according to a given protocol, necessary to assess the velocity beyond which it is useless to fluidize, because the discharge time of the reactor remains the same.

In case of fluidization of binary mixtures, the curve of fluidization has not the same behavior of mono-disperse case. The transition from fixed bed to fluidized bed

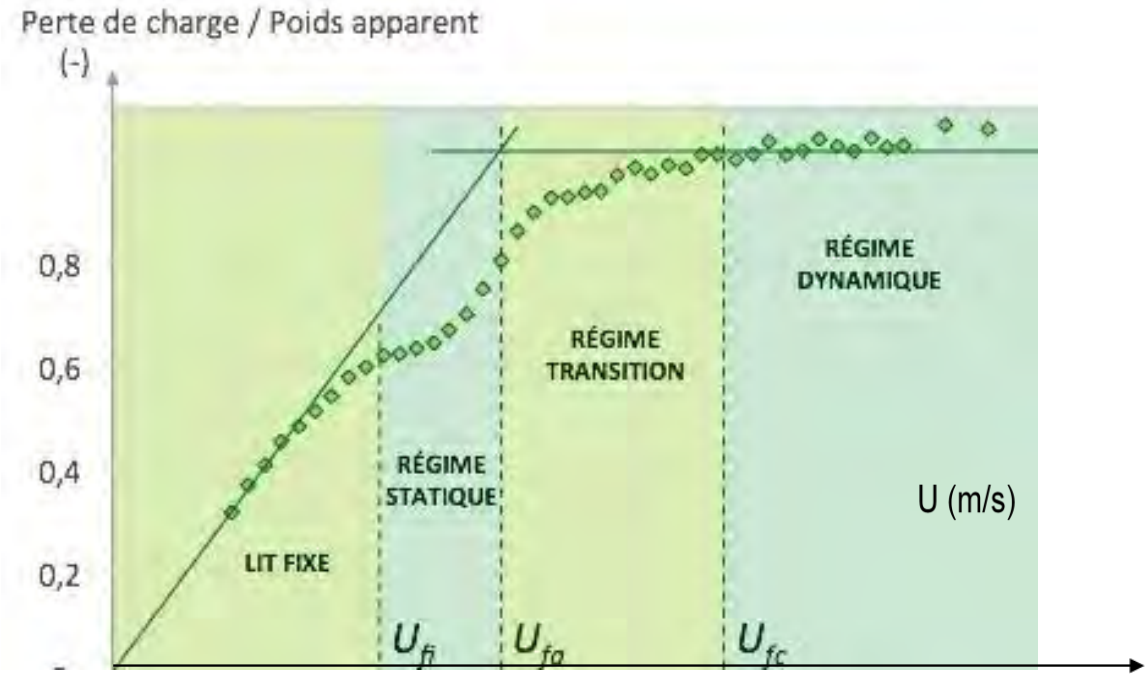

Figure 6.1 Different fluidization regimes in a binary mixture

(dynamic regime) does not occur at a unique velocity value. The transition occurs gradually; increasing the superficial gas velocity increases the gas pressure drop in the following order:

1. fixed bed, ($U<U_{fi}$),
2. steady state ($U_{fi} <U <U_{fa}$),
3. transition regime ($U_{fa}<U <U_{cf}$),
4. dynamic regime ($U> U_{cf}$).

It is possible to determine experimentally the value of complete fluidization velocity, as explained in the following. This value depends of the percentage of coarse particles present in the mixture.

It has been performed the identical experimental protocol to determine the complete fluidization velocity for each mixture.

The protocol is the following: at the beginning the superficial gas velocity is set at 9.5 times the minimum fluidization velocity; every three minutes of fluidization the velocity is lowered until it reaches half of the minimum fluidization velocity.

A significant number of data has been obtained. Experimental data, captured at 10 Hz by a computer work-station, have been evaluated an average every three minutes.

It has been possible to fill in a table containing values processed by the system of superficial gas velocity and of pressure of first pressure sensor.

At beginning the value of P1 is constant and close to the theoretical maximum value. Subsequently, its value decreases and it is possible to recognize the transition from dynamic regime to transition regime. This value is U_{cf} , determined experimentally. The velocity of complete fluidization is assumed as the velocity corresponding to the point of intersection between the straight line interpolating the pressure values measured under the condition of transition regime and the interpolating data relating to the fully fluidized bed. Further increases the superficial velocity of the fluidizing gas does not imply variations in the measured pressure.

Table 6.1 Trend of P1 as a function of effective velocity

Effective velocity (m/s)	P1 (mbar)	Effective velocity (m/s)	P1 (mbar)
0.488	30.519	0.219	30.680
0.454	30.615	0.189	30.446
0.419	30.715	0.155	28.149
0.386	30.733	0.125	25.189
0.356	30.789	0.090	20.339
0.322	30.819	0.057	14.135
0.287	30.736	0.026	7.656
0.257	30.712		

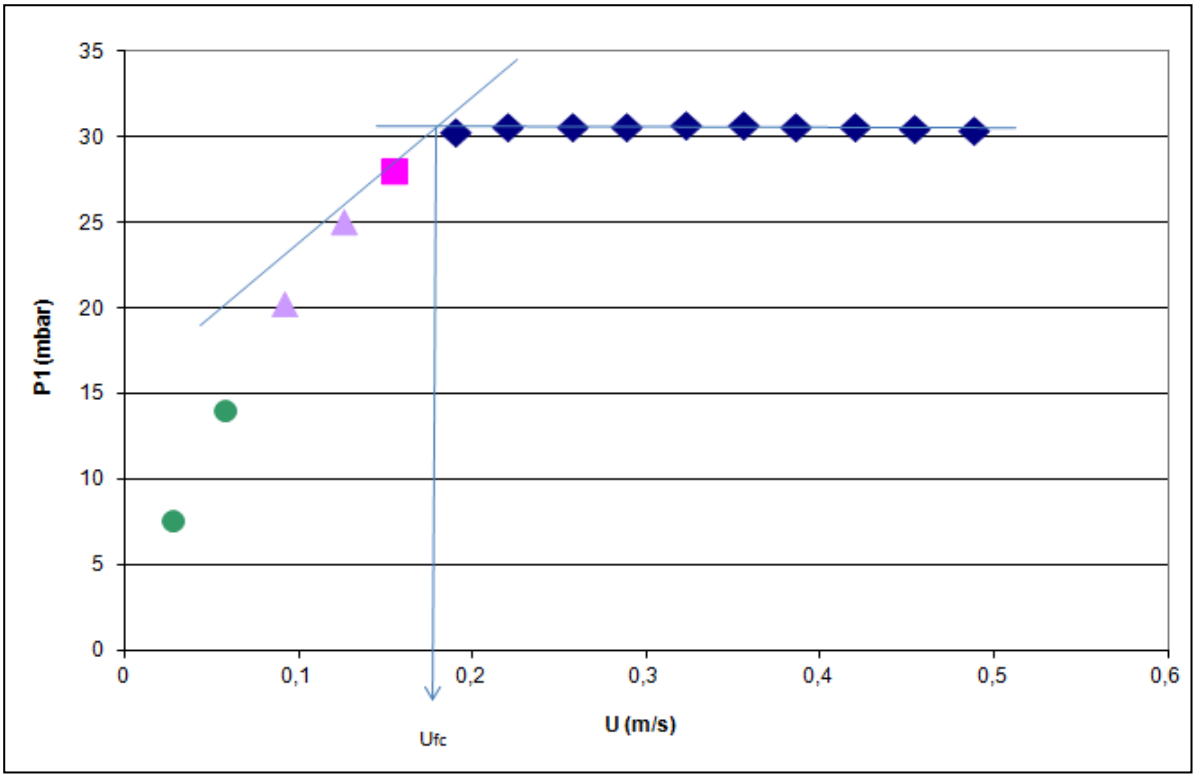

Figure 6.2 Determination of the velocity value at complete fluidization in a mixture containing 75% of coarse particles

The measurement has been made for mixtures; in case of mono-disperse's value the U_{cf} matches with the value of U_{mf}, as expected. The trend that is obtained is a nonlinear function, whose value of U_{cf} is strongly influenced by the percentage of

coarse particles put in the mixture. The results obtained are enclosed in the following table.

Table 6.2 Experimental U_{cf} in mixture

% coarse particle	Ucf (exp) m/s
0	0.19
25	0.176
50	0.08
75	0.055
100	0.053

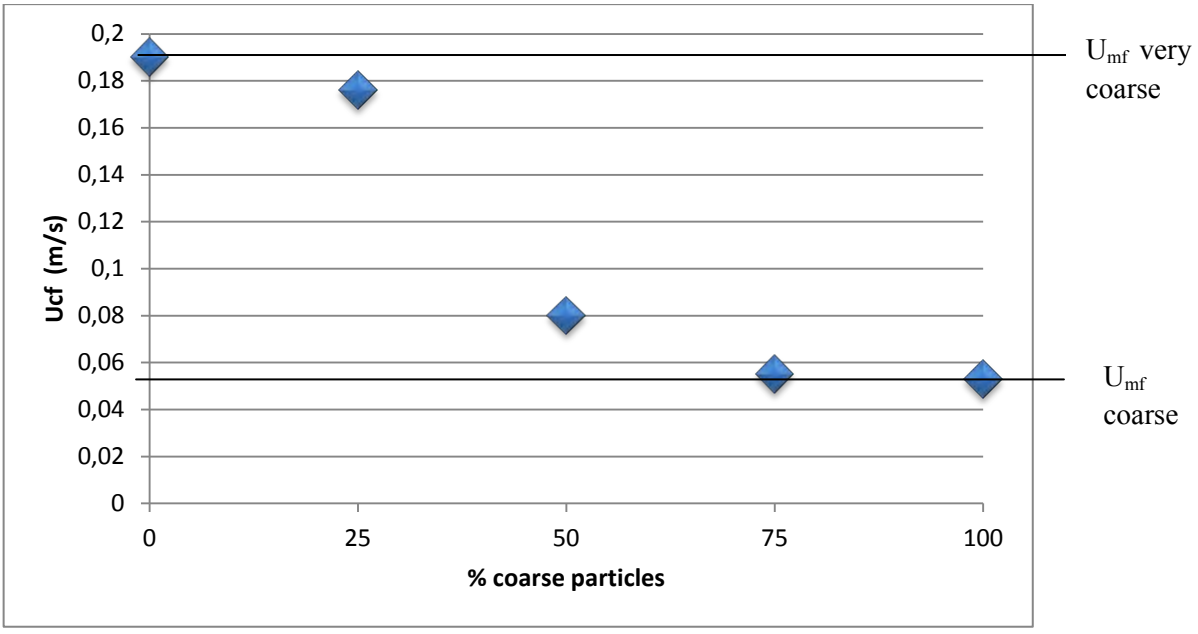

Figure 6.3 Experimental U_{cf} in mixture

The value of complete fluidization velocity is strongly influenced by the percentage of coarse particles put in the mixture, especially for the mixture containing 50% of smaller particles. However, we can notice that for mixture of 25% and 75% the value of U_{cf} is very close to the nearest mono-disperse's value.

6.1 Discharge time

We have been carry out the discontinuous experiments, to study the elutriation phenomenon. It naturally leads to a not stationary condition within the reactor due to the removal of the finest particles. Working with a batch process is often not a benefit to the economy of the process, the time scale extends and requires qualified staff. It is more complex for computer simulations, typically carried out at steady state.

It has been possible to carry out six different experiments to determine the discharge time as a function of superficial gas velocity in the mono-disperse case.

The experiments use 2.5 kg of coarse particles.

It has been performed the same protocol each time.

The first step has been a short fluidization period, t=3 minutes, at the value of 5 times U_{mf} .

The next seven minutes the bed is fluidized each time at different velocity. Each time the velocity is greater than the terminal settling velocity found with the equation of Wen and Yu.

Table 6.3 Determination of discharge time

Effective velocity (m/s)	**Time (s)**
2.257	33
2.182	43
2.107	60
2.032	103
1.957	142
1.807	605

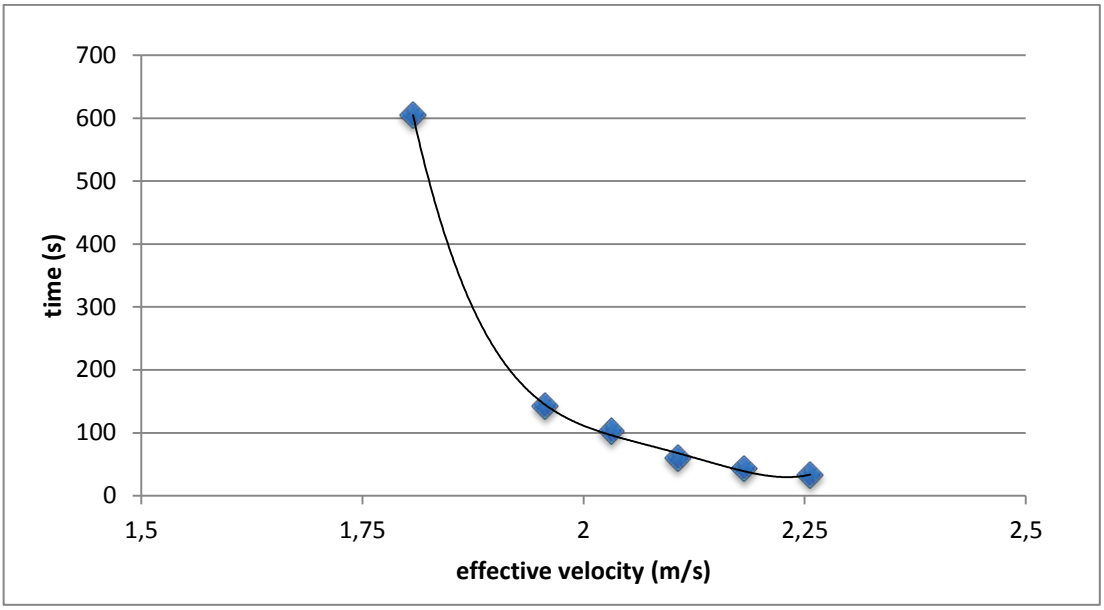

Figure 6.4 Determination of discharge time

The start time has been established by the loss of 5% of the mass of powder inside the column, corresponding to a decrease of 5% of the average value of P1.

The final instant that has determined the discharge time, known the initial total mass of powder, has been defined by the recovery of 95% of mass of the particles.

It is possible to introduce a new definition of velocity: the *choking velocity*. For velocities larger than this value it is useless to increase the volumetric flow rate of gas, because the discharge time becomes constant. In these experiments the value of choking velocity is 2.2 m/s. For velocities lower than the terminal settling velocity it is impossible to drag all the particles and the discharge time becomes infinite.

7 CHAPTER SEVEN

ELUTRIATION: EXPERIMENTS

In this chapter the occurrence of elutriation is analyzed in detail. Known that entrainment is a complex process, we conducted experiments in a batch mode to evaluate the ability and the rate of the reactor to empty.
After a steady state had been achieved, the elutriated powders were diverted and collected by a sampling container and then weighed. Finally, we took some samples to evaluate the particle size distribution after the entrainment.

The experiments

Elutriation of fines from a fluidized bed refers to particle ejection into and transport throughout the freeboard.

The motion of the whole flow of particles has been evaluated by conducting experiments with mixtures and evaluating the performance of elutriation of the smaller particles. To evaluate the accuracy of the experiments, two experiments have been conducted for each mixture. At the end of each experiment the powder that was in the recovery column has been recovered and weighed. The same protocol has been used for each experiment.

To ensure a good mixing between particles, the first step has been a short fluidization period, t=3 minutes, at the value of 5 times U_{mf} .
The next ten minutes the bed has been fluidized at a velocity greater than the terminal settling velocity of coarse particles found with the equation of Wen and Yu.

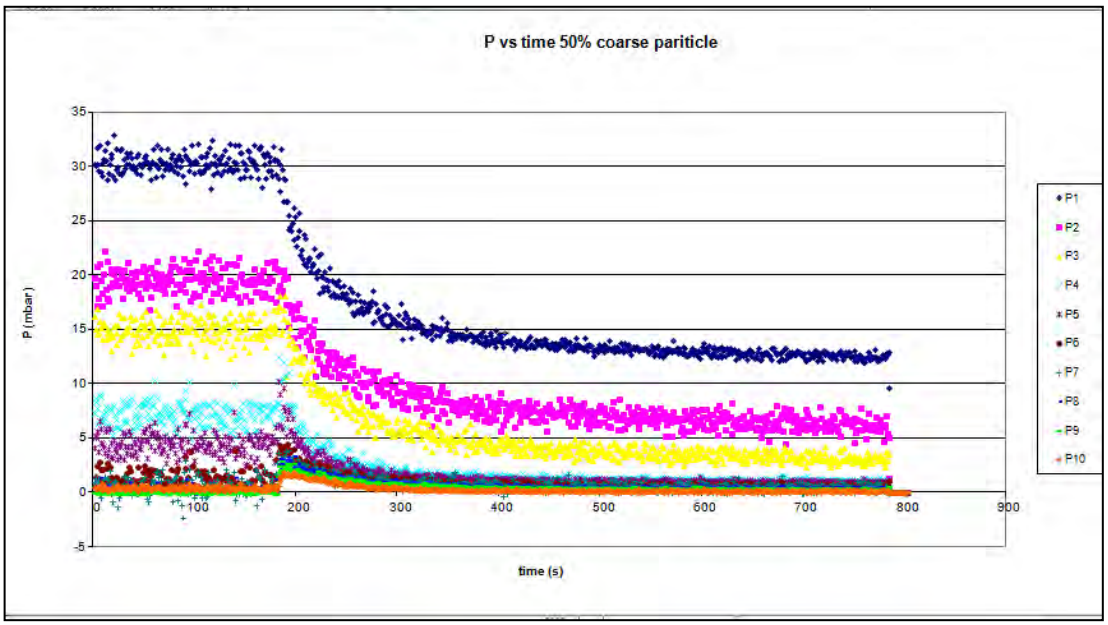

Figura 7.1 Pressure recorded by sensors in the case of 50% of coarse particles

At the beginning, for low values of velocity that ensure a good mixing, the average pressure recorded assumes a value approximately constant for each pressure sensor. The P1 sensor (at the bottom) records a value of pressure equal to the weight of the bed per unit of section. Subsequently, at a much higher value of the fluidization velocity, all the average values of pressure decrease. At the end, when finer particles have been elutriated from the reactor, the average values of pressure remains constant.

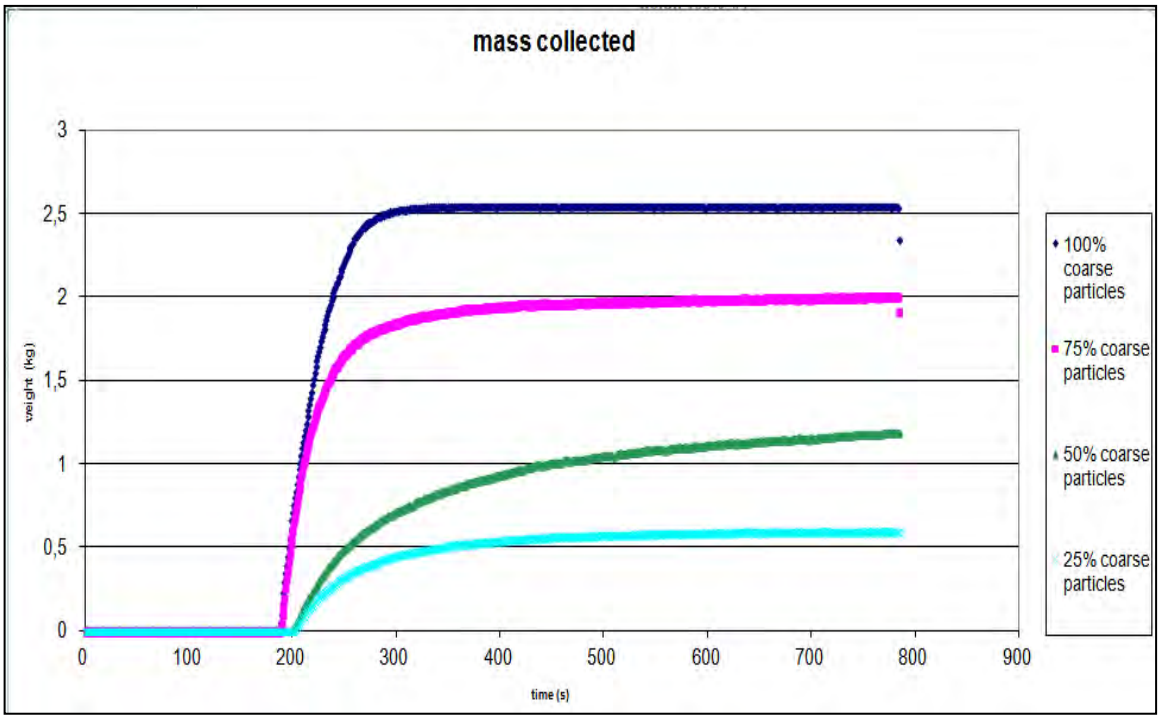

Figure 7.2 Mass of particles collected in four different experiments of binary mixture

The figure 7.2 shows that at the end of each experiment the recovered powder was equal to the maximum recoverable, both for the mixtures than for the case of mono-disperse finer particles. We can also note the absence of the curve of the case of mono-disperse larger particles. As expected, it was not possible to recover these particles because the effective gas velocity was below that terminal settling velocity of larger particles.

The maximum velocity of fluidization has been higher than the terminal settling velocity of smaller particles and lower than the terminal settling velocity of very coarse particles.

During this batch mode of operation, known in each case the percentage of coarse particles in the mixture, it has been possible to determine that the mass fraction of entrained solids has been always close to the hypothesized value, maximum theoretical value recoverable.

7.1 Particle Size Distribution in mixture

To assess how the presence of larger particle influenced the behavior of finer ones it has been decided to measure the particle size distribution of the particles collected after elutriation. In the recovery column three samples were taken at different heights which were subsequently analyzed.

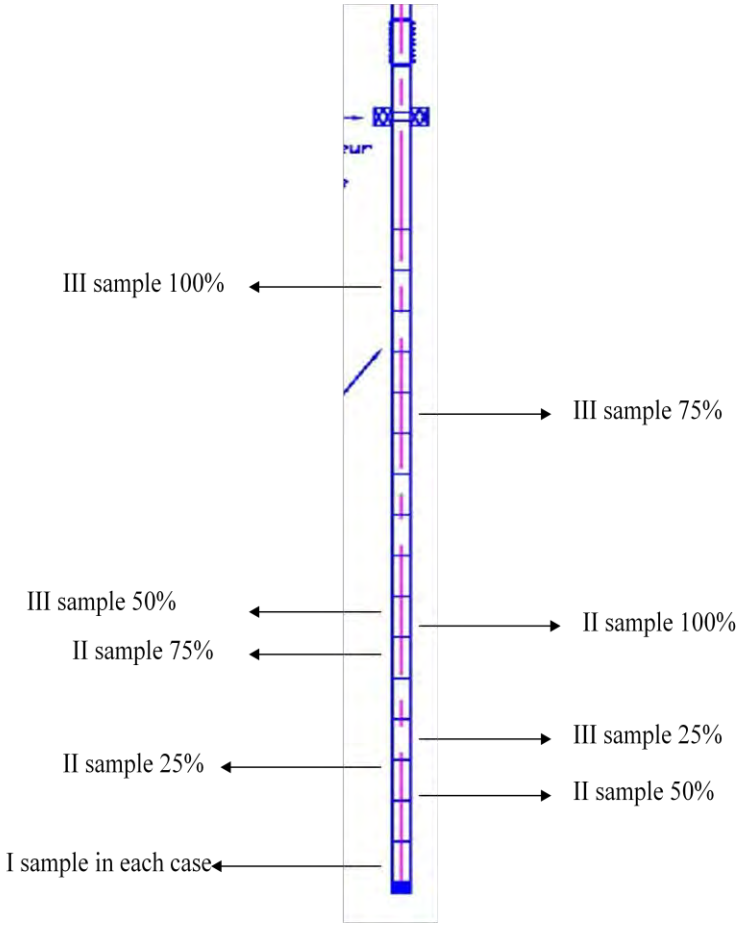

Figure 7.3 Position of samples

Table 7.1 Summary of granulometry of samples

% coarse particles	D (0.1)	D (0.5)	D (0.8)	D (0.9)	D (1)	D [3.2]
100%	182,96	250,74	308,98	343,11	525,16	243,281
	179,65	246,31	303,08	339,42	525,16	238,889
	203,69	277,09	339,17	375,92	610,99	269,513
75%	165,85	244,95	317,48	360,8	538,58	234,065
	176,29	243,35	300,64	337,23	525,16	235,887
	199,55	273,22	336	372,86	610,99	265,54
50%	177,54	255,14	324,62	366,14	610,99	245,235
	182,88	251,85	311,73	347,06	525,16	244,222
	186,03	253,07	309,48	345,89	525,16	245,855
25%	190,57	263,27	327,23	365,58	610,99	255,419
	182,02	249,16	307,33	341,45	525,16	241,909
	208,17	282,18	345,17	384,04	595,77	272,389

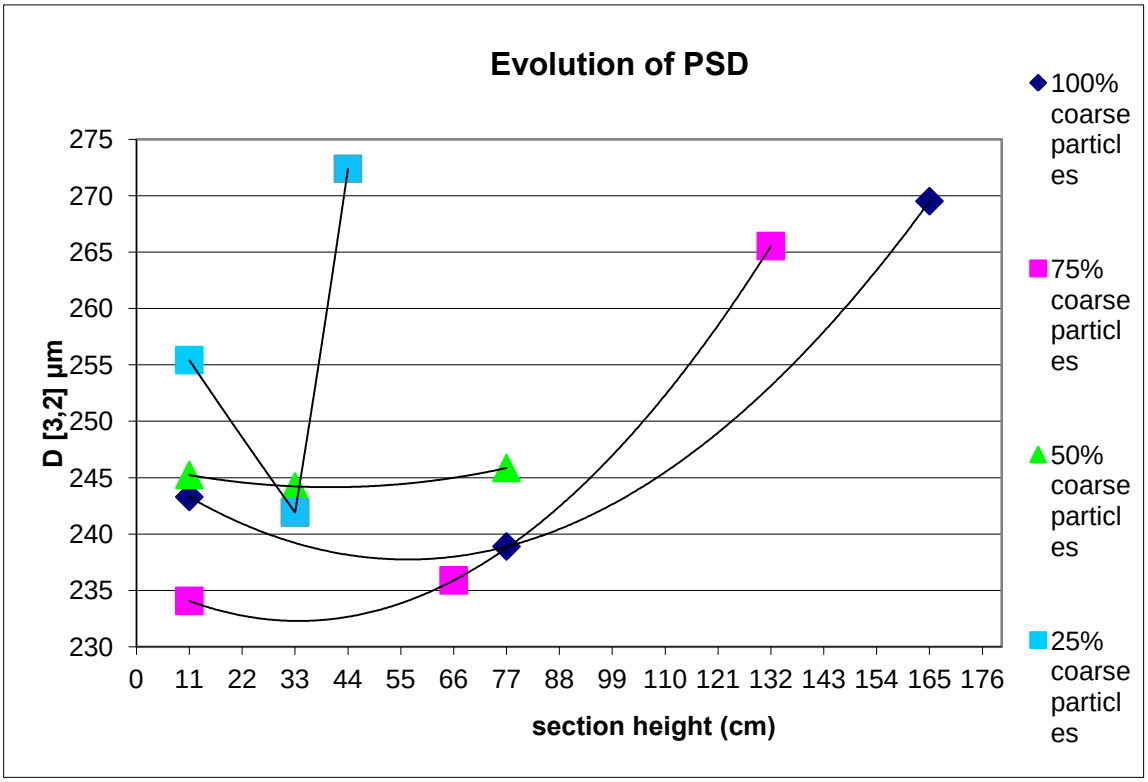

Figure 7.4 Evolution of PSD at different height and % of smaller particles

The particular trend of PSD, where smaller particles accumulate in the middle of the collected bed, is probably due to the particle size distributions of individual mono-disperse case that for some intervals overlap.

8 CHAPTER EIGHT

CIRCULATING FLUIDIZED BED AND FUTURE PROSPECTS

The term circulating fluidized bed, commonly abbreviated CFB, has been in common usage since the mid-1970s, although the origins of the technology date back to the 1940s for catalytic processes (Squires, 1994) and to the 1960s for gas–solid processes (Reh, 1971). The term implies two complementary characteristics for gas–solid systems:

1. A configuration where particles, entrained at a considerable flux from a tall main reactor or ‘‘riser,’’ are separated efficiently from the carrying fluid, usually external to the reactor, and returned to the bottom of the riser, forming a recirculation loop for the particles. Individual particles circulate around this loop many times before leaving the system, whereas the fluid passes through only once. A typical setup is shown schematically in Fig. 8.1.

2. Operation at high superficial gas velocity (typically 2–12 m/s) and high particle flux (typically 10–1000 kg/m2s) so that there is no distinct interface in the riser between a dense bed and a dilute region above. Contacting is therefore carried out at gas velocities beyond the bubbling, slugging and turbulent fluidization flow regimes, residing instead in a higher velocity flow regime—fast fluidization, dense suspension upflow, or dilute pneumatic conveying.

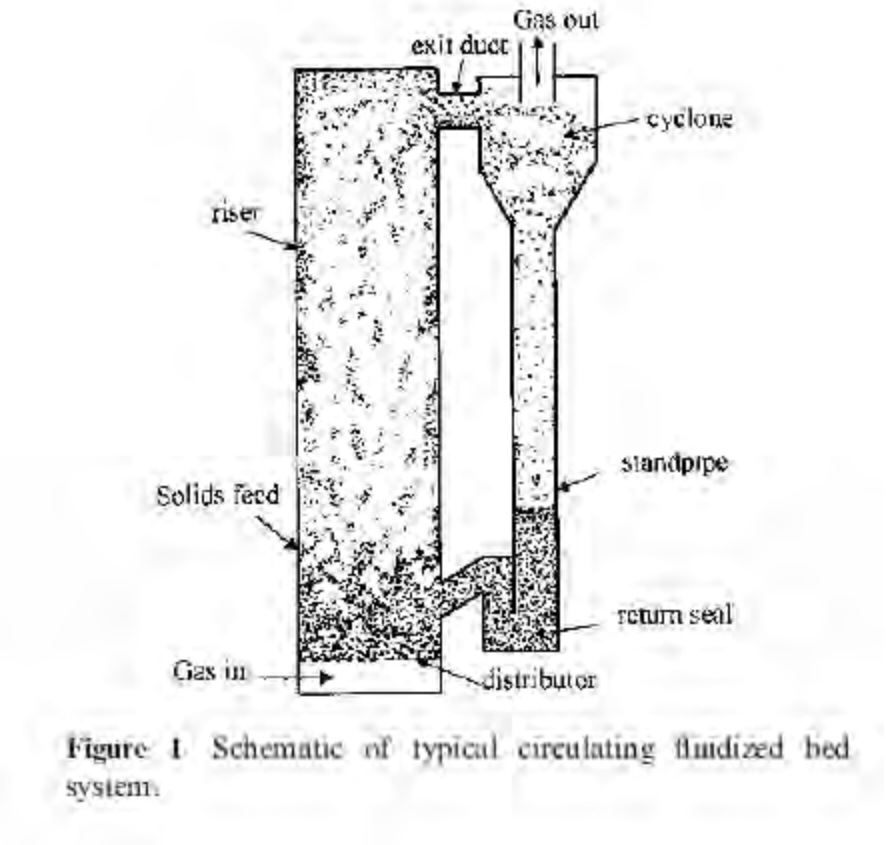

Figure 1 Schematic of typical circulating fluidized bed system.

Figure 8.1 Schematic of typical Circulating Fluidized Bed

In recent years, the term circulating fluidized bed has also been used for liquid–solid systems and gas– liquid–solid (three-phase) systems.

It is possible to summarize the advantages and disadvantages of circulating fluidized beds.

Advantages

- High gas throughputs
- Limited backmixing of gas
- Long and controllable residence time of particles
- Temperature uniformity, without ‘‘hot spots’’

- Flexibility in handling particles of widely differing sizes, densities, and shapes
- Effective contacting between gas and particles
- Lack of bypassing of gas with minimal mass transfer limitations
- Opportunity for separate and complementary operation (e.g., catalyst regeneration or particle cooling) in the return loop

Disadvantages often include:

- Need for very tall vessel: small scale CFB processes are therefore seldom viable
- Substantial backmixing of solid particles
- Internals (e.g., baffles, heat transfer surfaces) not viable because of wear/attrition
- Wall wastage sometimes a serious problem
- Suspension-to-surface heat transfer less favorable than for low-velocity fluidization
- Lateral gradients can be considerable
- Losses of particles due to entrainment.

Many applications of circulating fluidized beds are listed in Table 8.1, together with key references.

These applications include solid-catalyzed gas reactions and gas–solid reactions, as well as physical operations.

While catalytic cracking and solid-fuel combustion are the predominant catalytic and gas–solid reaction applications, respectively, there are also a number of other processes where the unique characteristics of circulating fluidized beds are being exploited.

Table 8.1 Major applications of Circulating Fluidized Bed

Table 1 Major Commercial Applications of Circulating Fluidized Beds

Application	Key References	Comments
Fluid catalytic cracking	Avidan, 1997; Sec. 8.1 of this handbook	Hundreds of units worldwide; mainstay of petroleum refining
Fischer–Tropsch synthesis	Shingles & McDonald, 1988; Steynberg et al., 1991; Matsen, 1997	Applied for many years as Synthol process in South Africa
Maleic anhydride	Matsen, 1997; Contractor, 1999	One commercial reactor in Spain
Combustion of coal, biomass, wastes, off-gases	Li and Zhang, 1994; Brereton, 1997; Lee, 1997; Basu, 1999; Plass, 2001	Widespread usage for power generation and boilers in Europe, North America, and Asia
Gasification	Hirschfelder & Vierrath, 1999; Plass, 2001	Commercial units gaining a foothold, especially in Europe
Calcination (e.g., of aluminium trihydrate and carbonates)	Reh, 1971, 1986; Schmidt, 1999	Lurgi units used widely
Catalyst regeneration	Chen et al., 1994	Applied in China
Roasting of ores	Dry & Beeby, 1997; Pienermann et al., 1992	Applied in Australia
Reduction of iron ore	Dry & Beeby, 1997; Husain et al., 1999; Plass, 2001	Lurgi plant in Trinidad
Smelter off-gas treatment	Hiltunen & Moyöhänen, 1992	One plant in Australia supplied by Ahlstrom
Flue gas dry scrubbing of HF, HCl, SO_2, dioxins, mercury, etc.	Graf, 1999; Mayer-Schwinning & Herden, 1999	Commercial units since the 1970s, primarily in Europe

If it is necessary for the industry to have a continuous process, the achievement of a steady state in laboratory experiments, using a recirculation process, allows an easier comparison with the results obtained by the numerical simulations.

Microwave sensors

Microwave attenuation techniques have been used to measure the solid concentration in pneumatic conveying by measuring the particle velocity and volume concentration (Yan, 1996). Solid particles within the pipeline absorb microwave energy and increase the attenuation between the microwave source and the detector.

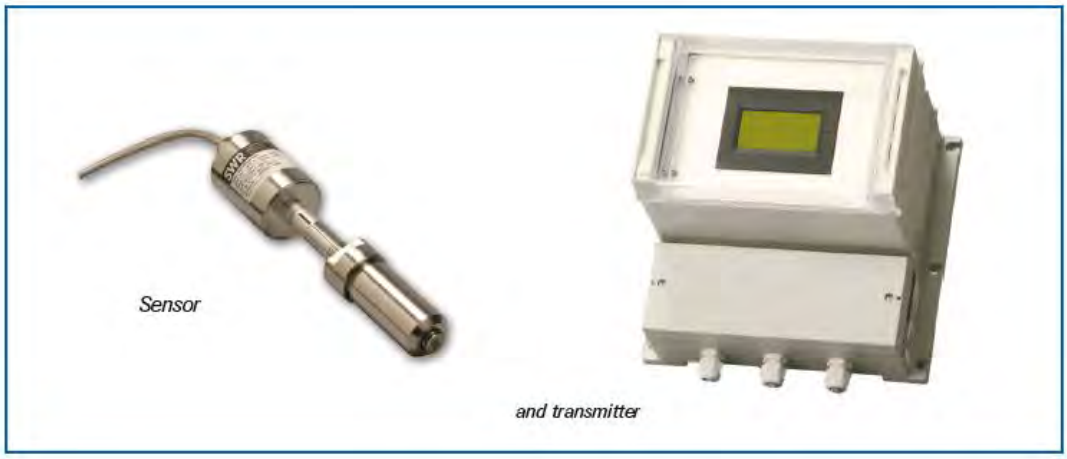

Figure 8.2 Microwave sensor and transmittor

The microwave sensor was supplied by the company SWR Engineering and it is used exclusively in metal piping. Based on Doppler effect, the solid velocity is obtained through the measured frequency difference between the signals emitted and reflected by the solid. Moreover, the amplitude of the received signal allows determining the solid concentration. This technology is non-intrusive, provides real-time online flow measurements and can be operated at high temperatures. The microwave signal varies linearly with the solids mass flow rate in the pilot. Hence, only one point will be sufficient to calibrate the microwave sensor in situ.

The recirculation column, which allows the powder to return to the primary column, has been put into operation and has given good performance. Due to time constraints has not been possible to calibrate the probe. Therefore it is no possible to do comparisons with data from the literature or with numerical simulations.

Future prospects provide to calibrate the probe, which allows to continuously monitor the transition of the particles in the top of the primary column, so as to verify the acquisition of continuous measurements, to improve the experimental results and to compare these with literature data and with numerical simulations.

In the future it will be possible to study the fluid dynamic behavior of different types of mixtures consisting of different particles than those considered in this study.

CONCLUSIONS

This is an experimental study on the expansion of the bed of granular solids and binary mixtures of solids with the goal of validating numerical simulations.

Hydrodynamic behavior of gas–solid flow in the bubbling fluidized beds depends upon the particle properties. In a system consisting of particles of equal density, but different sizes, the bigger particles tend to remain at the bottom of the bed.

With increasing gas velocity the total pressure drop of bed increases in the fixed bed obeying Ergun's Law.

When the superficial gas velocity equals the minimum fluidization velocity the bed pressure drop exactly balances the buoyant weight per unit cross-sectional area of the bed.
It is possible to distinguish a linear trend in the variation of pressure in the bed.

Void ratio increases with increasing of mass fraction of small particles.

The results obtained through the experiments are in agreement with the results obtained by numerical simulations and are in agreement with the predictions of data literature and from previous studies.

In case of binary mixtures the complete fluidization velocity decreases with increasing of the mass fraction of small particles. The mixture with a higher percentage of coarse particles is fluidized at lower velocity. The results obtained through the experiments are in agreement with the results obtained by numerical simulations. As also shown by the numerical simulations, the reactor had a high degree of mixing and there was no appreciable segregation.

In poly-disperse case, each time, the modeling predicts a behavior inside the reactor similar to the data obtained experimentally. The height of the expanded bed obtained through numerical simulations and experiments is always almost the same. We can recognize as the limits of the model the difficulties in modeling the behavior of the powders in the freeboard.

The study of elutriation shows that at the end of each experiment the recovered powder was equal to the maximum recoverable, both for the mixtures than for the case of mono-disperse finer particles. As expected, it was not possible to recover larger particles.

The elutriation rate is higher for mono-disperse case of smaller particles.

To assess how the presence of larger particles influenced the elutriation of finer particles it has been decided to measure the PSD of the particles collected.

The particular trend of PSD found is not intuitive; probably it is due to the particle size distributions of the individual mono-dispersed cases that for certain intervals overlap.

In the future it will be possible to study the fluid dynamic behavior of different types of mixtures consisting of particles different than those considered in this study.
Investigate the behavior of the mixtures will be useful for designing more performing and innovative reactors.

Appendix

Laboratoire de Génie Chimique
UMR 5503 CNRS-UPS-INPT/ENSIACET
Campus Labège
4 allée Emile Monso - BP 84234
31030 Toulouse cedex 4
Tél. : +33 (0) 534 323 600
Fax : +33 (0) 534 323 700
http://lgc.inp-toulouse.fr

MASTERSIZER 2000

Rapport d'analyse

Echantillon: coarse_particles_treated
SOP: VS_billes_verre_vib70%_pres2.5bars
Mesuré: jeudi 10 avril 2014 15:30:14
Mesuré par: Sébastien Wahl
Analysé: jeudi 10 avril 2014 15:30:53
Sample bulk lot ref: 123-ABC
Source Resultat: Mesure
Pression : 2.5 Bars **% Vibration :** 70

Nom Particule: verre
Accessoire: Scirocco 2000 (A)
Modèle d'analyse: Analyse standard
Sensitivity: Normal
RI Particule: 1.530
Absorption: 0.1
Gamme de Mesure: 0.308 to 1092.000 um
Obscuration: 0.92 %
Dispersant:
RI Dispersant: 1.000
Résiduel Pondéré: 2.201 %
Modif. de Résultat: Désactivé

Concentration: 0.0073 %Vol
Span : 0.765
Uniformité: 0.24
Type de Distribution: Volume
Surface Spécifique: 0.0252 m²/g
Surface Weighted Mean D[3,2] ou Diamètre de Sauter : 237.725 µm
Vol. Weighted Mean D[4,3] ou Diam Moyen pondéré (dm) : 257.973 µm
Densité: 1.000

d(0.1): 170.370 µm **d(0.5):** 247.797 µm **d(0.9):** 360.013 µm

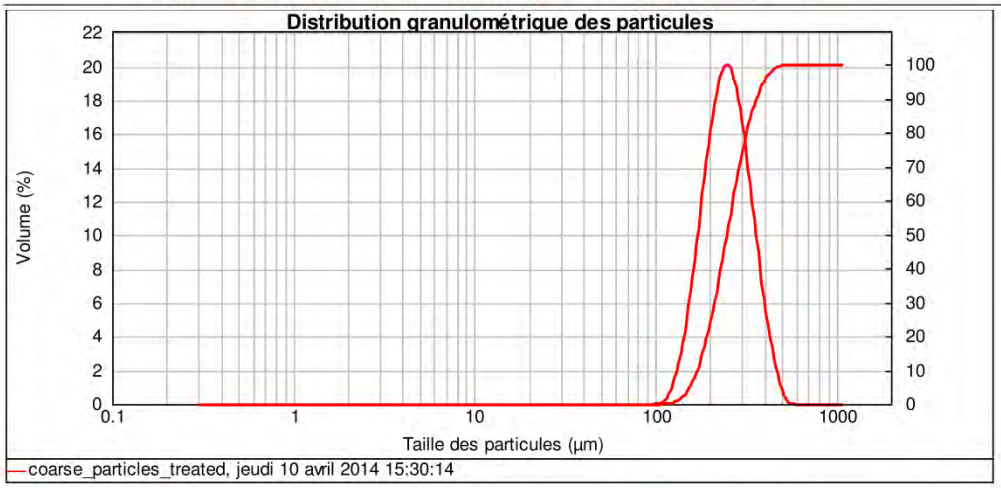

Taille (µm)	Volume en %	Taille (µm)	Volume en %	Taille (µm)	Volume en %	Taille (µm)	Volume en %	Taille (µm)	Volume en %	Taille (µm)	Volume en %
0.010	0.00	0.085	0.00	0.615	0.00	5.209	0.00	44.102	0.00	373.369	5.80
0.012	0.00	0.099	0.00	0.717	0.00	6.068	0.00	51.371	0.00	434.912	1.96
0.014	0.00	0.100	0.00	0.835	0.00	7.068	0.00	59.839	0.00	506.599	0.08
0.016	0.00	0.115	0.00	0.972	0.00	8.233	0.00	69.702	0.00	590.102	0.00
0.018	0.00	0.134	0.00	1.133	0.00	9.590	0.00	81.191	0.00	687.369	0.00
0.021	0.00	0.156	0.00	1.320	0.00	11.171	0.00	94.574	0.01	800.669	0.00
0.025	0.00	0.182	0.00	1.537	0.00	13.012	0.00	110.163	0.63	932.643	0.00
0.029	0.00	0.211	0.00	1.790	0.00	15.157	0.00	128.321	3.07	1086.372	0.00
0.034	0.00	0.246	0.00	2.085	0.00	17.656	0.00	149.472	7.73	1265.439	0.00
0.039	0.00	0.287	0.00	2.429	0.00	20.566	0.00	174.110	13.69	1474.023	0.00
0.046	0.00	0.334	0.00	2.830	0.00	23.956	0.00	202.809	18.57	1716.987	0.00
0.054	0.00	0.389	0.00	3.296	0.00	27.904	0.00	236.238	19.93	2000.000	
0.062	0.00	0.453	0.00	3.839	0.00	32.504	0.00	275.177	17.06		
0.073	0.00	0.528	0.00	4.472	0.00	37.861	0.00	320.535	11.48		
0.085	0.00	0.615	0.00	5.209	0.00	44.102	0.00	373.369			

Operator notes:

Figure 1 Analysis report of Particle Size Distribution of coarse particles

AccuPyc 1330 V2.04N
n° de série : 3355

RAPPORT DE DENSITE ET DE VOLUME

Nom de l'échantillon : He-Billes de verre coarse 1

début : 11 / 04 / 14 13 : 02 : 59
fin : 11 / 04 / 14 13 : 29 : 50

masse initiale : 12.1000 g

température : 20.1 °C
taux d'équilibre : 0.050 psig/min

nombre de purges : 30

insert : aucun
facteur de calibration : 1.000000

volume de cellule : 11.5591 cm3
volume d'expansion : 9.3351 cm3

procédé	volume (cm3)	déviation (cm3)	densité (g/cm3)	déviation (g/cm3)	temps écoulé (h:min:s)
1	4.8723	0.0001	2.4834	-0.0001	0 : 12 : 51
2	4.8718	-0.0004	2.4837	0.0002	0 : 14 : 23
3	4.8712	-0.0010	2.4840	0.0005	0 : 15 : 56
4	4.8721	-0.0001	2.4835	0.0000	0 : 17 : 28
5	4.8722	-0.0001	2.4835	0.0000	0 : 19 : 01
6	4.8725	0.0003	2.4833	-0.0002	0 : 20 : 33
7	4.8724	0.0002	2.4834	-0.0001	0 : 22 : 06
8	4.8724	0.0002	2.4834	-0.0001	0 : 23 : 38
9	4.8728	0.0005	2.4832	-0.0003	0 : 25 : 11
10	4.8726	0.0003	2.4833	-0.0002	0 : 26 : 43

volume moyen : 4.8722 cm3
densité moyenne : 2.4835 g/cm3

écart-type : 0.0004 cm3
écart-type : 0.0002 g/cm3

Figure 2 Analysis report of Helium Pycnometry of coarse particles

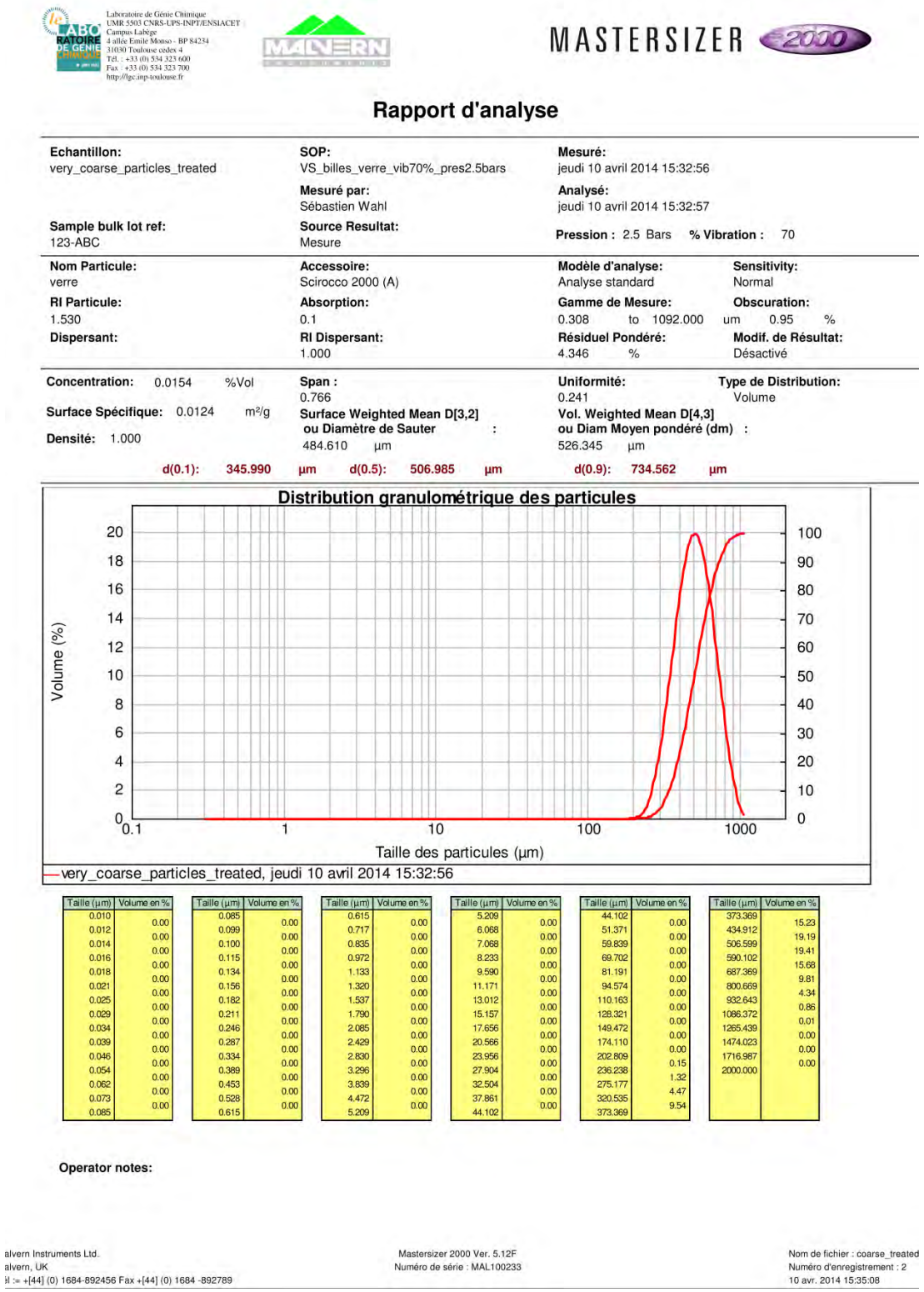

Taille (µm)	Volume en %	Taille (µm)	Volume en %	Taille (µm)	Volume en %	Taille (µm)	Volume en %	Taille (µm)	Volume en %	Taille (µm)	Volume en %
0.010	0.00	0.085	0.00	0.615	0.00	5.209	0.00	44.102	0.00	373.369	15.23
0.012	0.00	0.099	0.00	0.717	0.00	6.068	0.00	51.371	0.00	434.912	19.19
0.014	0.00	0.100	0.00	0.835	0.00	7.068	0.00	59.839	0.00	506.599	19.41
0.016	0.00	0.115	0.00	0.972	0.00	8.233	0.00	69.702	0.00	590.102	15.68
0.018	0.00	0.134	0.00	1.133	0.00	9.590	0.00	81.191	0.00	687.369	9.81
0.021	0.00	0.156	0.00	1.320	0.00	11.171	0.00	94.574	0.00	800.669	4.34
0.025	0.00	0.182	0.00	1.537	0.00	13.012	0.00	110.163	0.00	932.643	0.86
0.029	0.00	0.211	0.00	1.790	0.00	15.157	0.00	128.321	0.00	1086.372	0.01
0.034	0.00	0.246	0.00	2.085	0.00	17.656	0.00	149.472	0.00	1265.439	0.00
0.039	0.00	0.287	0.00	2.429	0.00	20.566	0.00	174.110	0.00	1474.023	0.00
0.046	0.00	0.334	0.00	2.830	0.00	23.956	0.00	202.809	0.00	1716.987	0.00
0.054	0.00	0.389	0.00	3.296	0.00	27.904	0.00	236.238	0.15	2000.000	
0.062	0.00	0.453	0.00	3.839	0.00	32.504	0.00	275.177	1.32		
0.073	0.00	0.528	0.00	4.472	0.00	37.861	0.00	320.535	4.47		
0.085	0.00	0.615	0.00	5.209	0.00	44.102	0.00	373.369	9.54		

Figure 3 Analysis report of Particle Size Distribution of very coarse particles

AccuPyc 1330 V2.04N
n° de série : 3355

RAPPORT DE DENSITE ET DE VOLUME

Nom de l'échantillon : He-Billes de verre very coarse 2

début : 11 / 04 / 14 17 : 14 : 31
fin : 11 / 04 / 14 17 : 40 : 14

masse initiale : 14.1551 g

température : 20.2 °C
taux d'équilibre : 0.050 psig/min

nombre de purges : 30

insert : aucun
facteur de calibration : 1.000000

volume de cellule : 11.5591 cm3
volume d'expansion : 9.3351 cm3

procédé	volume (cm3)	déviation (cm3)	densité (g/cm3)	déviation (g/cm3)	temps écoulé (h:min:s)
1	5.6807	-0.0001	2.4918	0.0000	0 : 12 : 31
2	5.6803	-0.0004	2.4920	0.0002	0 : 13 : 58
3	5.6808	0.0001	2.4917	-0.0001	0 : 15 : 25
4	5.6806	-0.0002	2.4919	0.0001	0 : 16 : 51
5	5.6805	-0.0003	2.4919	0.0001	0 : 18 : 17
6	5.6808	0.0001	2.4917	-0.0001	0 : 19 : 45
7	5.6809	0.0002	2.4917	-0.0001	0 : 21 : 13
8	5.6813	0.0006	2.4915	-0.0003	0 : 22 : 40
9	5.6809	0.0002	2.4917	-0.0001	0 : 24 : 07
10	5.6806	-0.0002	2.4918	0.0000	0 : 25 : 35

volume moyen : 5.6807 cm3
écart-type : 0.0003 cm3
densité moyenne : 2.4918 g/cm3
écart-type : 0.0001 g/cm3

Figure 4 Analysis report of Helium Pycnometry of very coarse particles

Nomenclature

C_d	drag coefficient	[-]
d[3,2]	Sauter mean diameter	[µm]
d_p	mean diameter	[µm]
Ga	Archimede Number	[-]
g	gravitational acceleration	[m/s^2]
Re	Reynolds Number	[-]
U_{mf}	velocity of minimum fluidization	[m/s]
U_{cf}	velocity of complete fluidization	[m/s]

Greek letters

α_p	solid ratio	[-]
ε	void ratio	[-]
ρ_p	density of solid	[g/cm^3]
ρ_g	density of gas	[g/cm^3]
µ	gas viscosity	[kg/m*s]

Bibliography

Ansart R., Detournaya M., Hemati M., Biomass vapogasification in Circulating Fluidized Bed: Study of hydrodynamic behavior at ambient temperature, Récents Progrès en Génie des Procédés, Numéro 104 – 2013

Bi H. T., Ellis N., Abba I. A., Grace J. R., A state-of-the-art review of gas-solid turbulent fluidization, Chemical Engineering Science 55 (2000) 4789-4825

Chase George G., SOLIDS NOTES 5, The University of Akron

Chirone R. e Scala F., Reattori a letto fluido e combustione di "opportunity fuels", Corso di Dottorato congiunto Polimi-Federico II Anacapri: 5-9 Ottobre 2009

Ganguly U.P., The Prediction of Critical Concentration in the Phenomenon of Elutriation of Solid from a Gas-Solid Fluidised Bed System, Indian Institute of Chemical Engineers Vol. 50 No. 2 April-June 2008, pp. 141-148

Geldart D., Powder Technology, 7 (It1731 2;~5).

Geldart D., in D. Geldart (ed.), Gas Fluidization Technology, Wiley, Chichester, UK, 1986.

Girimonte R. and Vivacqua V., The expansion process of particle beds fluidized in the voids of a packing of coarse sphere, Powder Technology 213 (2011) 63–69

Huilina Lu, He Yuronga, Dimitri Gidaspowb, Yang Lidana, Qin Yukun, Size segregation of binary mixture of solids in bubbling fluidized beds, Powder Technology 134 (2003) 86– 97

Kunii D. and Levenspeil O., Fluidization Engineering, 2ed., Butterworth-Heineman, Boston, 1991

Kunii and Levenspiel, J. Chem. Eng. Japan, 2, 84, (1969)

Lewis et. al., Chem. Eng. Prog. Symposium Series, 58, 38, 65, (1962)

Ma X. and Kato K., Effect of interparticle adhesion forces on elutriation of fine powders from a fluidized bed of a binary particle mixture, Powder Technology 95 (1998) 93- 101.

Menegus M., MicroGasic: Hydrodynamic study and design of a microreactor for gas-solid reactions in absence of catalyst support material, Tesi di Laurea Magistrale in Ingegneria Chimica, Università di Padova. (2014)

Merrick D. and Highley J., AIChE Symp. Ser., 137 (1974) 366.

Milioli F.E. and Foster P.J., Entrainment and elutriation modelling in bubbling fluidized beds, Powder Technology 83 (1995) 233-243

Moreau T., Projet de fin d'étude - Elutriation en lit fluidisé, INP- ENSEEIHT (2014).

Smolders K. and Baeyens J., Elutriation of fines from gas fluidized beds: mechanisms of elutriation and effect of freeboard geometry, Powder Technology 92 (1997) 35—46

Tasirin S.M. and Geldart D., Entrainment of FCC from fluidized beds a new correlation for the elutriation rate constants K_i , Powder Technology 95 (1998) 240-247

Wen C.Y. and Chen L.H., AIChE J., 28 (1982) 117.

Wen-Ching Yang, Handbook of fluidization and fluid-particle systems (2003)

Yan Yong, (1996), Mass flow measurement of bulk solids in pneumatic pipelines. IOP Science, 16 September, pp. 1687-1706.

Yun-Long Han, Chien-Song Chyang, Wei-Min Hsiao, Kuo-Chao Lo, Effect of fines hold-up in the freeboard on elutriation from a fluidized bed, Journal of the Taiwan Institute of Chemical Engineers 42 (2011) 120–123.

Siti web

http://lgc.inp-toulouse.fr/ (ultimo accesso: 24/02/2015)